A SEISMIC STRATIGRAPHIC ANALYSIS AND PETROLEUM SYSTEM CHARACTERIZATION OF THE CRETACEOUS SEQUENCE IN CENTRAL WALVIS BASIN, OFFSHORE NAMIBIA

A THESIS SUBMITTED IN PARTIAL FULFILMENT

OF THE REQUIREMENTS FOR THE DEGREE OF

MASTER OF SCIENCE IN PETROLEUM GEOLOGY

OF

THE UNIVERSITY OF NAMIBIA

BY

ESTER LINEEKELA MEGAMENO DAVID

201136562

OCTOBER 2025

MAIN SUPERVISOR: DR. INNOCENT MUCHINGAMI (UNIVERSITY OF NAMIBIA)

CO-SUPERVISOR: DR. MARTIN HARRIS (UNIVERSITY OF NAMIBIA)

ABSTRACT

The Walvis Basin, situated along Namibia's passive margin, has long been recognized for its hydrocarbon potential. With only nine (9) exploration wells drilled to date, the Walvis Basin remains relatively under-explored. The uncertainties concerning the occurrence and preservation of mature source rocks and good reservoir lithofacies in the northern and central parts of the Walvis Basin remains exploration risks. This study aims to address this gap by carrying out a seismic stratigraphic analysis of 2D seismic data and well data in the Central Walvis Basin. Nine (9) seismic intervals (SI) have been identified spanning Late Jurassic to Cretaceous based on seismic character and well log data corresponding to the evolutionary stages of the Walvis Basin. The proposed seismic sequence stratigraphy model suggests source, reservoir, trap, and seal rocks in both the syn-rift and post-rift successions of the study area. Source rocks deposited in Cenomanian to Turonian period, based on well data and modelling the Cenomanian-Turonian marine source rock is in the early maturity window with total organic carbon (TOC) levels ranging from 0.63% to 5.86%, averaging at 2.02% in the study area. Additionally, marine Aptian/Albian oil-prone source rocks were identified by prominent distinct parallel high-amplitude horizons which can also serve as a seal rock. Potential Reservoir rocks were identified in Cenomanian and Santonian levels and at Upper Campanian/Maastrichtian indicating the potential for hydrocarbon exploration in the basin. This research will contribute to our understanding of the geological history of the Walvis Basin and offer valuable insights into its hydrocarbon potential, hydrocarbon prospectivity of this underexplored basin.

Key words: hydrocarbon, lithofacies, seismic stratigraphy, petroleum system, Walvis Basin

LIST OF CONFERENCES PROCEEDINGS

I have presented the preliminary results of this study at the following conference:

A seismic stratigraphic analysis and petroleum system characterization of the Cretaceous sequence in Central Walvis Basin, Offshore Namibia

Ester LM David[1]*, I. Muchingami[1], M. Harris[1], Alina Narubes[2], Wina Shipo[2]

[1]Department of Geoscience, Faculty of Agriculture, Engineering and Natural Sciences, University of Namibia, Keetmanshoop, Namibia

[2]National Petroleum Corporation of Namibia, Upstream Exploration and Production, Petroleum House, 1 Aviation Road, Windhoek, Namibia

*E-mail: esterdavid82@gmail.com

1. Poster presentation at the AAPG Conference 22-24 July 2024

TABLE OF CONTENTS

LIST OF TABLES

LIST OF FIGURES

LIST OF ABBREVIATIONS AND/ OR ACRONYMS

2D - Two Dimensional

3D -Three Dimensional

FSST- Falling Stage Systems Tracts

HST- Highstand System Tract

HC- Hydrocarbon

LST- Lowstand System Tract

MD- Measured Depth

MFS- Maximum Flooding Surface

NAMCOR- Namibia Petroleum Corporation of Namibia

PSTM- Prestack Time Migration

RSL- Relative Sea Level

SDRs- Seaward Dipping Reflectors

SI- Seismic Intervals

TS- Transgressive Surface

TOC- Total Organic Content

TST- Transgressive System Tract

UNAM- University of Namibia

ACKNOWLEDGEMENTS

I would like to express my deepest gratitude to everyone who has supported and contributed to the completion of this thesis. First and foremost, I thank the Almighty God for His unwavering guidance, wisdom and strength throughout this journey and making this research possible. His blessings have been a source of inspiration and perseverance. I am profoundly grateful to my supervisors, Dr. Innocent Muchingami and Dr. Martin Harris, whose expertise, patience, and encouragement have been invaluable. Your insightful feedback and continuous support have greatly enriched this work. I am deeply thankful to NAMCOR for providing access to the research data and for their invaluable support with special thanks to Alina Narubes, Wina Shipo, Frieda Thomas, Lohmeier Eiseb, Erich Nepembe and Lucas Shifeleni. Your willingness to assist me with my research has been instrumental in the success of this thesis. You really made time to assist me. I would also like to extend my appreciation to Schlumberger for providing the Petrel 2022 software essential to this research. Your generous provision of the software, along with the comprehensive training on its use, has greatly facilitated the progress of my work. I also extend my sincere appreciation to Petrofund for providing the financial support that made this research possible. Your generosity has been crucial in allowing me to focus on my studies and complete this thesis.

To my friends and classmates Justina Hamalwa and Joel Iyambo, thank you for your team spirit and encouragement. Your support has made this challenging journey both enjoyable and rewarding. Special thanks go to my friend Reginalda Joseph who has helped me during my struggles and made me understand better and never left me alone even in the hardest situations, I really appreciate you for everything you have gone through for me. I would also acknowledge the unwavering support of my mother Alina Paulus who continuously encouraged me, I thank the Lord for you.

Thank you all for being a part of this significant achievement.

DEDICATION

I dedicate this thesis to Abba Father, my Lord and Savior. I dedicate it to my dearest mother, Alina Paulus. I would also like to dedicate it to my friendship and the NAMCOR geoscience department. Thank you for your endless support.

DECLARATIONS

I, Ester LM David, declare hereby that this study is a true reflection of my own research, and that this work, or part thereof has not been submitted for a degree in any other institution of higher education.

I, Ester LM David, grant The University of Namibia the right to reproduce this thesis in whole or in part, in any manner or format, which The University of Namibia may deem fit, for any person or institution requiring it for study and research; providing that The University of Namibia shall waive this right if the whole thesis has been or is being published in a manner which the University deemed fit.

Irrespective of the above, access to the thesis and parts thereof must be restricted according to the Confidentiality Agreement with NAMCOR and the University of Namibia.

Ester LM David Date: October 2025

CHAPTER 1: INTRODUCTION

1.1 Background of the study

Synthesis of seismic facies analysis, sequence and seismic stratigraphy assist in reconstructing basin paleogeography and provide the insights to a basin's petroleum system (Futalan et al., 2012). Seismic stratigraphy emerged in the 1970s with the work of Vail et al. (1975) and has evolved to sequence stratigraphy with the incorporation of outcrop and well data (Van Wagoner et al., 1990). Recognition of seismic stratigraphic units and their seismic facies, such as reflection configuration, frequency, and amplitudes, allow for prediction of lithofacies intervals that may contain source, seal, and reservoir lithologies (Joseph, 2020; Mitchum Jr et al., 1977; Yugyè et al., 2022) . In addition, high-resolution 3D seismic data has a potential to allow for the characterisation of major petroleum elements and processes. Seismic-stratigraphic data, may provide detailed information on seismic prospects concerning the structural, stratigraphy, and lithology (Taner et al., 1979; Van Wagoner et al., 1990). For example, the trapping systems within the Kribi-Campo sub-basin have been described using seismic analysis (Le, 2012). Also, Chongwain et al. (2021) identified various sequences and seven facies units in the Douala basin, Cameroon through seismic analysis. Joseph (2020) predicted lithofacies in the Lüderitz Basin based on seismic stratigraphic interpretation. The results were the identification of several source, reservoir and seal rock units in both, the syn-rift and post-rift from their lithology model. The prospective nature for oil and gas exploration within the offshore Cenozoic of the Kribi-Campo sub-basin highlighted potential source rocks, reservoirs, seals, and structural and stratigraphic traps throughout the studied seismic intervals (Yugyè et al., 2022). The Walvis Basin (Figure 1) is under-explored (Tower Resources PLC, 2020). There is limited information on the lithofacies in the northern and central part of Walvis Basin. This could be related to lack of well control between Welwitschia-1 well and the 1911 (1911/10-1 and 1911/15-1) wells in the graben itself. Furthermore, the Welwitchia-1 well, situated south of the Dolphin Graben did not penetrate any source and reservoir rocks. There are two proven source rocks in the Walvis Basin and offshore Namibia: the Aptian-Albian and Cenomanian-Turonian source rocks (Kuhlmann et al., 2011). Both source rocks have been penetrated by Wingat-1 and Murombe-1 (Kukulus, 2004), located in Walvis Basin further south of the basin. The Aptian-Albian source rock was not penetrated by the two 1911 wells in the Dolphin Graben (Kukulus, 2004). On the other hand, well 1911-15-1 indicated some oil shows. Thus, the presence of mature source rocks, reservoir lithofacies and their preservation in northern and central Walvis Basin is not well established. The uncertainty around mature source rocks, reservoir facies, and their preservation is due to a combination of insufficient well control, immature source rock conditions in drilled areas, seismic resolution limits, and uncertainties in burial and tectonic history. This study follows the methodology by Futalan et al. (2012) on seismic facies analysis and sequence stratigraphy to give an insight of the petroleum system of the Walvis Basin. The understanding of the seismic stratigraphy and of source and reservoir lithologies in the northern and central Walvis Basin may resuscitate interest in exploring the basin further and may potentially encourage new dataset acquisition and further drilling campaigns in the basin.

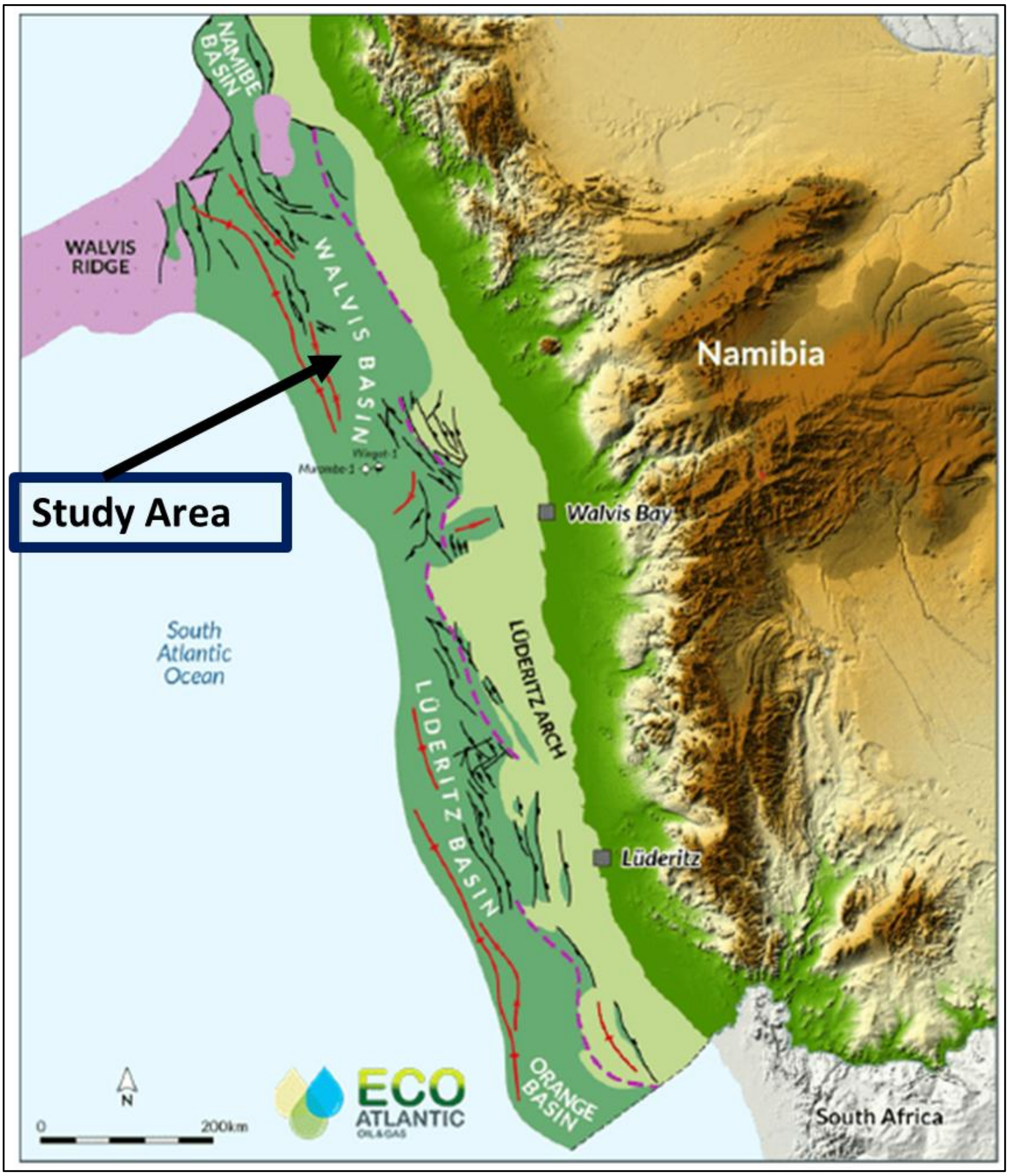

Figure 1: Regional geographic map of Namibia with the main hydrocarbon exploration basins. The study area in the Walvis Basin is indicated. Image modified from Eco Atlantic Oil & Gas. (n.d.).

1.2 Exploration history of the offshore basins, Namibia

Exploration for hydrocarbons within the Namibian shelf margin began in the late 1960"s and the first successful discovery was the Kudu Gas Field discovered in 1974 (The Namibian, 2014). In 1987-1988 Swakor, the predecessor company of the present

National Oil Company (NAMCOR), drilled two additional wells (Kudu-2 and 3) in the Kudu Gas Field. The Kudu-2 well was not tested but Kudu-3 proved the existence of a major gas field. The proven hydrocarbons were an asset in Namibia's first licensing round.

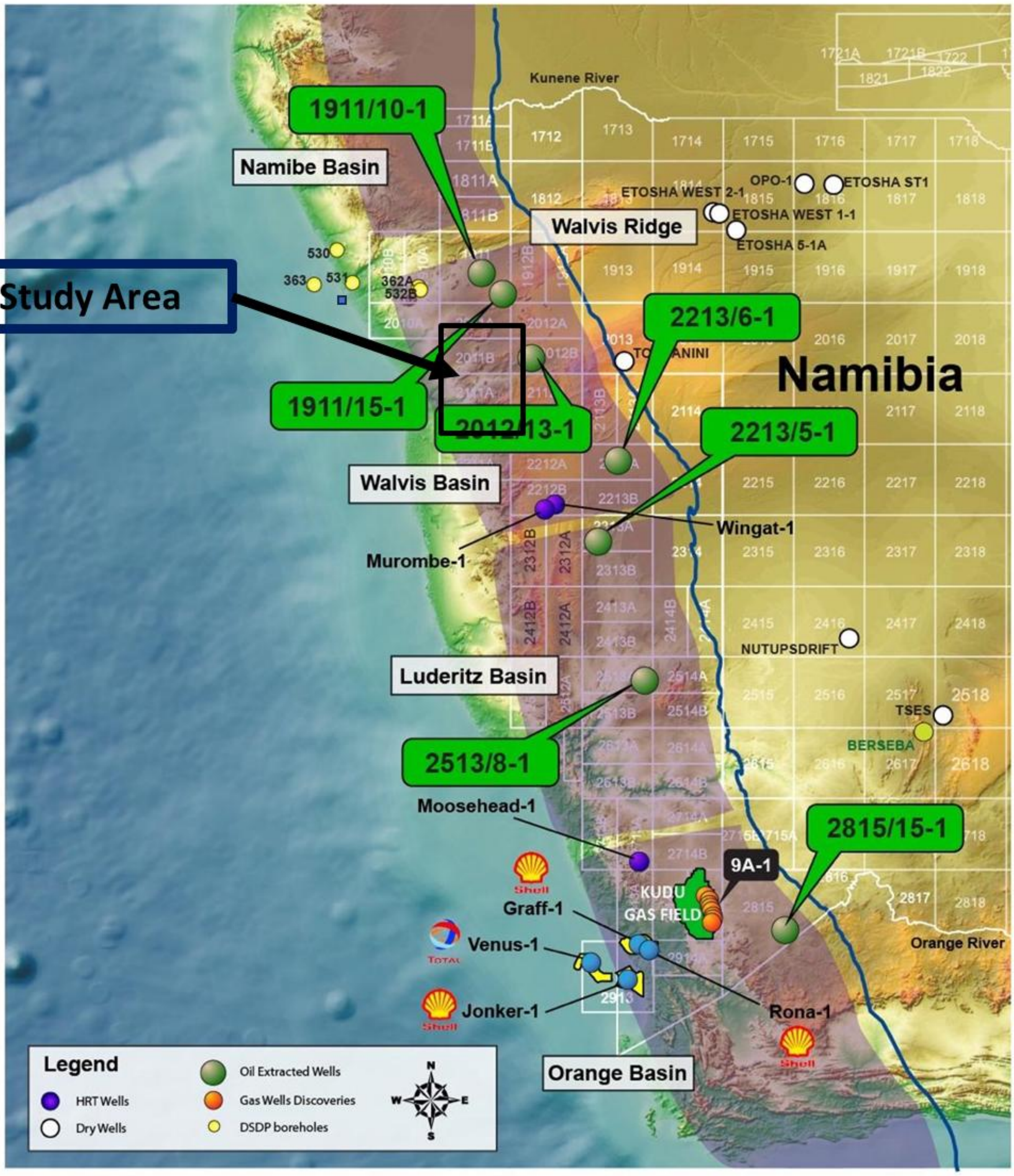

Figure 2: Location map of the onshore and offshore Namibia showing offshore hydrocarbon basins and wells with and without hydrocarbon discoveries along with gas/oil shows. Image modified from BrazilPetroleumStudies (2022)

The Aptian source rock has been penetrated by discovery well of the Kudu field. This Aptian source rock is believed to be deposited in a restricted marine environment which is both oil and gas prone (Bray et al., 1998). The Aptian source rock is about 140 meters thick and overlying thinner source rock intervals from the Barremian period. The average Total Organic Carbon (TOC) content of approximately 2% (Bray et al., 1998).

The overlying source rock of the Cenomanian to Turonian periods appears to be absent in the Kudu field. However, this source rock correlated with a stratigraphic the equivalent oil-prone source rock of the Orange Basin (Kukulus, 2004). Moreover, there is a promising Cretaceous-age marine source rock with good oil-producing potential identified in the Walvis Basin. The Cenomanian-Turonian source rock has an average TOC of 5%, and although the shales are not yet thermally mature, there's potential for hydrocarbon generation given sufficient burial depth (Kukulus, 2004).

The syn-rift interval may also have potential as a source rock. It is believed that during the initial stages of rifting, lacustrine environments formed, which could have preserved organic rich oil-prone claystones. In the South African Orange Basin, oil-prone lacustrine source rocks are found in the Hauterivian syn-rift section (Hartwig, 2014). Proven reservoirs include the pre-rift sandstones and carbonates, syn-rift continental sandstones, Aptian carbonate and late Cretaceous/Tertiary turbidites. These reservoirs have been identified in Well 1911/15-1 in the Walvis Basin, with porosity ranging from 15% to 31%. Specifically, the Campanian-Maastrichtian deep marine turbidites having a porosity of 16-25%, while the deep marine fans have a very good porosity ranging from 26% to 31% (NAMCOR E&P, 2016).

The Kudu Field has Early Cretaceous transitional reservoirs. These reservoirs consist of aeolian sandstones intercalated with volcaniclastic deposits, marine sandstones, and shaley limestones. With an average net thickness of 50 meters and porosity reaching up to 20%, they hold significant potential for development (NAMCOR E&P, 2016). In addition, there are prospective deep-water reservoirs in the form of basin floor fans located above the mid-Aptian and upper Santonian unconformities in the deeper northern sections of the Kudu Field. Furthermore, marginal marine and fluvial sand deposits within the syn-rift section may contribute to the reservoir potential (Spectrum, 2012).

Comparately to the Orange Basin and the Lüderitz Basin also have potential reservoirs spanning the Lower Cretaceous, Upper Cretaceous, and likely into the Palaeogene periods. A thick layer of shallow marine shelf sand has been proven in well 2513/8-1, ranging from 1363 to 1408 meters deep, with an average porosity of 17%. Evidence of a regional top seal exists at the Aptian-Albian shale level, indicated by significant pressure differential between the over-pressured Aptian-Albian carbonates and the younger, normally pressured sandstones (NAMCOR E&P, 2016). Mesozoic intra-formational shale, occurring at various depths, has been identified as potential cap rock in the Walvis Basin. Additionally, in the Orange Basin, the Barremian and Aptian source rocks may act as seal rocks (NAMCOR E&P, 2016).

Onshore, there are two extensive Neoproterozoic or Early Cambrian Basins: the Owambo Basin in the north and the Nama Basin in the south rocks (NAMCOR E&P, 2016). Most onshore exploration and stratigraphic wells are relatively shallow and have not fully explored the onshore potential. Nonetheless, both offshore and onshore exploration efforts have confirmed a functioning petroleum system, having multiple reservoirs, source rock, trap, and seal sequences. This research will delve into Namibia's petroleum systems, focusing on how these various elements interact to define proven and potential petroleum systems.

1.3 Statement of the problem

Seismic sequences as well as the different seismic facies units that occur in the Walvis Basin are yet to be unraveled hence the petroleum system elements and processes of this basin are yet to be properly understood. This study will help identify the major petroleum system elements within the basin.

1.4 Aims and Objectives

The aim of this study is to evaluate the seismic stratigraphy and characterize the petroleum system of the Cretaceous sequence of the central Walvis Basin.

To achieve this, the following specific objectives were met:

a) Identify and delineate the key seismic sequences of the study area.

b) To understand the depositional environment.

c) Establish the various seismic facies

d) Identify the major petroleum system elements within the basin (source, reservoir, traps and seal)

CHAPTER 2: LITERATURE REVIEW

2.1 Regional Geology of the South Atlantic Passive Margin

The South Atlantic continental margins resulted from the break-up of Gondwana, with Antarctica separating from Africa and South America at around 155 Ma (Koopmann et al., 2014; Light et al., 1993). According to Wen et al (2019) the South Atlantic conjugate passive continental margin basins from south to north include Falkland Plateau, Colorado, Punta Del Este, Santos, Campos, Potiguar, and Guyana basins in the west side and Outeniqua, Southwest African Coastal, Kwanza, Lower Congo, Gabon, and Liberia basins in the east side. These basins experienced multiple tectonic evolution stages from Mesozoic to Cenozoic. The opening of the South Atlantic took place in the Early Cretaceous with suggested opening ages ranging between 137 and 126 Ma (Light et al., 1993). The central and southern regions of the Namibian margin show typical volcanic margin elements, including thickened original oceanic crust, seaward dipping reflectors, and dense lower crust with high velocity, extending beneath the rift zone formed during Early Cretaceous seafloor spreading (Figure 3). The Namibian and South African continental margin is one of the examples of a volcanic margin and forms the conjugate to the volcanic margin of the Pelotas Basin of the southern Brazil (Miller, 2008). It consists of a post-rift progradational-aggradational wedge with a thickness (3-5km) comprising clastic sedimentary rocks of post-rift sediments overlying a rifted continental basement.

During the breakup of Gondwana four basins were formed. Namibia has four offshore basins, namely, the Orange Basin, which is down South of Namibia, extending into South Africa; the Lüderitz Basin, the Walvis Basin and the Namibe Basin. These basins were formed during the Late Jurassic to Early Cretaceous breakup of Gondwana (Blaich et al., 2011). It consists of a post-rift progradational-aggradational wedge with a thickness (3-5km) clastic sedimentary rocks of post-rift sediments overlying a rifted continental basement.

Seismic stratigraphic analysis of the post-rift mega sequence of the Namibian passive continental margin has enabled depositional features to be interpreted in terms of the likely controls on their formation (Bagguley & Prosser, 1999). Five megasequences define offshore Namibia on the basis of reflection terminations and geometries, each of these is related to a major phase of basin evolution which involve the early stages of rifting and the subsequent opening of the South Atlantic (Bagguley & Prosser, 1999). The rift megasequence is overlain by a transitional megasequence, which in turn is overlain by the main post-rift succession.

Bagguley and Prosser (1999) interpreted the seismic channel forms on the inner shelf as incised valleys that were formed during a fall in relative sea level. A series of shallow mounded features was also identified on the shelf, which the Bagguley and Prosser (1999) interpreted as palaeo dune fields, or carbonate build-ups, or longshore clastic mounds. The outer shelf and upper slope positions reveal canyon and channel forms.

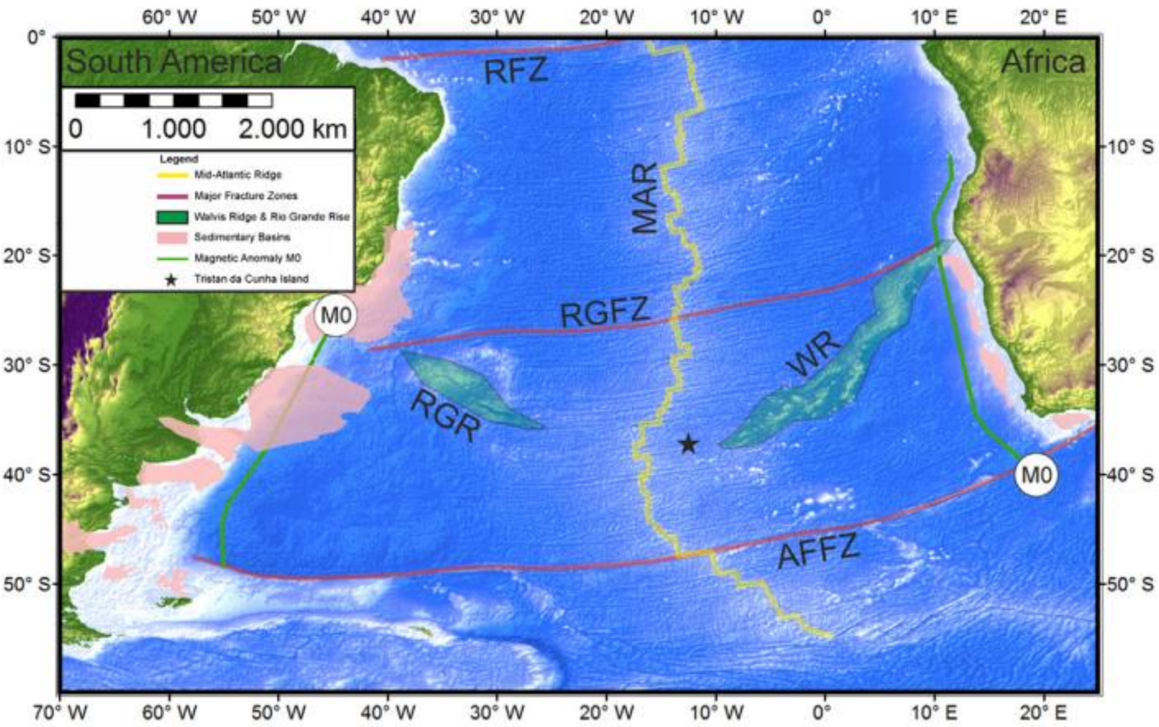

Figure 3: Regional map of the South Atlantic. It shows volcano-tectonic characteristics along the Namibian and Southern African margin between the Agulhas Falkland Fracture Zone (AFFZ) and the Rio Grande Fracture Zone (RGFZ). The map shows the distribution of the sedimentary basins in the study area on the Namibian and Southern African margin (South to North: Outeniqua Basin; Orange Basin; Lüderitz Basin; Walvis Basin)(Koopmann et al., 2014)

Many rifted continental margins experienced massive, transient magmatic activity during final continental breakup and initial sea floor spreading. An example is the margin off Namibia which formed during the Early Cretaceous breakup of South America and Africa (Gladczenko et al., 1998; Light et al., 1993). The distance from the mid-ocean ridge to the boundary between continental and oceanic crusts, the continuous and gradual accumulation of oceanic crust offers chronological markers for the ocean floor (Serratt et al., 2022). Conversely, volcanic passive margins are characterized by an abundance of volcanic rocks exhibiting wedge shaped geometries known as seaward-dipping reflectors (SDRs), these rocks slope towards the deeper parts of the ocean and are commonly identified through seismic reflection surveys. Their presence compliance the delineation of the oceanic-continental crust boundary. Some magnetic anomalies, previously attributed to regular vertical oceanic crust, are associated with SDRs (Hall et al., 2018). However, these SDR-related magnetic anomalies are not indicative of age; rather, they result from variations in magnetic susceptibility rather than remanent magnetism (Hall et al., 2018).

According to Chauvet et al (2021) and Gladczenko et al (1998) the volcanic character of the southwest African margin has a prominent seaward dipping reflectors (SDRs) which characterize the outer margin off Namibia south of the Walvis Ridge. The SDRs continue south along the African margin and present on the conjugate Brazil-Argentine margin. The SDR has three main structural types (inner, outer and intermediate) that can be distinguished based on both the curvature of the reflectors and the topography displayed at their downdip terminations. The influence of the pre-rift inheritance, the mode of rifting and the coeval mantle dynamics may explain this global architecture (Chauvet et al., 2021). On the Walvis Ridge, the SDR wedge is narrower, ∼50-km-wide, farther south; the SDR wedge is capped there by a smooth, locally faulted surface (Gladczenko et al., 1998).

2.2 Tectono-stratigraphy of the Namibia Passive Margin

The tectono-stratigraphy of the Namibian Passive Margin refers to the sequence of rock layers that formed in the region in response to the tectonic and sedimentary processes. The passive margin of Namibia, like other passive margins, had undergone a series of tectonic events that have influenced the deposition of sedimentary rocks

(Holtar & Forsberg, 2000). The passive margin offshore Namibia consists of an eastern Graben Province separated by an extensive coast-parallel Central Half-Graben by a Medial Hinge Line.

According to Chauvet et al (2021), Gladczenko et al (1998), Kukulus (2004) and Light et al (1993); stratigraphy of Permian to Recent sediments can be subdivided into five main tectono-stratigraphic sequences:

Table 1: Stratigraphy of Permian to Recent sediments is subdivided into five main tectono-stratigraphic sequences

Tectono-stratigraphic sequences	
Thermal Sag	Horizon P-sea floor
Transitional	Horizon Q-P
Syn-rift II	Horizon R-Q
Syn-rift I	Horizon T-R
Basin & Range	Horizon W-T

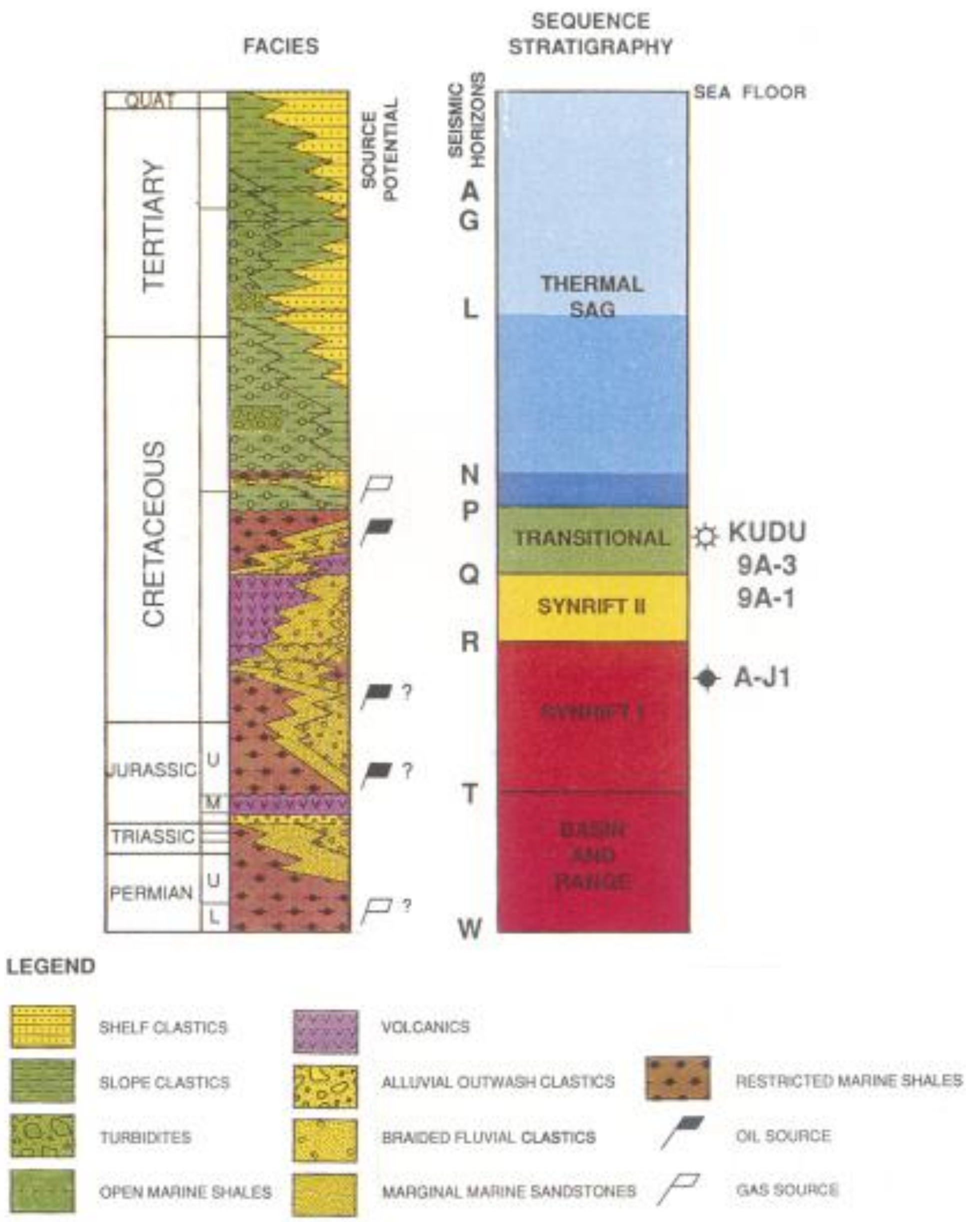

Figure 4: Stratigraphy and seismic horizons of the African margin, derived from (Light et al., 1993)

2.2.1 Basin and Range Province

Basin and Range formed during the Permian to Early Jurassic Pre-rift presented as horizon T. The stratigraphy and structure of Basin and Range continental clastics and acid to intermediate volcanics, are comparable with the Basin and Range Province in the US (Light et al., 1992, 1993). This megasequence is interpreted as a Late Jurassic angular unconformity. The Basin and Range Megasequence consists essentially of the Karoo formations as defined within the main Karoo Basin in South Africa and Karoo Basin in southern Namibia. Seismic reflectors along a broad north/south-trending belt, west of the Medial Hinge Line, display a complex pattern of high amplitude, discontinuous, irregular and hummocky events, probably representing arid continental deposits with aeolian dunes, fluvial sands, lower energy braidplain silts and shales, and extensive tracts of subaerially extruded lavas (Light et al., 1993).

2.2.2 Syn-rift I

The tectonic history of the passive margin of Namibia began with the breakup of the supercontinent Gondwana during the Jurassic and Early Cretaceous periods, around 140 million years ago. This rifting process created tensional forces that led to the development of rift basins. These basins gradually subsided and filled with sediment as the Atlantic Ocean opened. Syn-rift I heralded the opening of the South Atlantic in the Early Cretaceous, when a new set of rift basins was localized offshore Namibia, west of the Basin & Range rift (Central Half-Graben) (Light et al., 1992, 1993). The Syn-rift I interval which is preceding Syn-rift II megasequence represents a wedge-shaped, generally westwards-thickening sequence, which pinches out at the Medial Hinge Line in the east, usually due to erosion (Light et al., 1993). It is developed in the northern part of Nambian margin (Kukulus, 2004). No wells in the Namibian offshore have penetrated this sequence, therefore facies interpretations are speculative (Light et al., 1993). Progradational and chaotic reflection patterns along the margins of many of these grabens indicate that elastic fans were developed marginally, and grade laterally and vertically into fluvial, braidplain and, perhaps, lacustrine sequences, marked by more regular, more continuous, and parallel reflectors (Light et al., 1993).

2.2.3 Syn-rift II

A second syn-rift event, Syn-rift II, developed in the northern part of offshore Namibia and was associated with widespread volcanism, related to the Walvis Ridge mantle plume (130-120 Ma)(Dingle, 1992; Dingle et al., 1983; Light et al., 1993). During the early stages of rifting, the region experienced the formation of rift basins, such as the Etendeka Basalts and Huab Basins. Huab Basins were characterized by the deposition of volcanic and sedimentary rocks. The Etendeka Basalts are prominent in Syn-rift II and represent the initial phases of volcanic activity associated with rifting (Ryberg et al., 2015). The Etendeka (Kaoko Group) Volcanics dated between 136 and 114 Ma(Light et al., 1993) are inter-bedded with aeolian and fluvial sands. Onshore, aeolian and wadi sandstones are inter-bedded with volcanics throughout the Kimmeridgian to Barremian interval (136-114 Ma) (Light et al., 1993), which indicates that climatic conditions had again become arid in Namibia. West of the Medial Hinge Line, seismic reflection characteristics in the Orange and Luderitz Basins have low amplitude, semi-continuous to discontinuous, sometimes wavy, with inter-bedded quieter and transparent zones (Light et al., 1993). Very low angle prograding units are sometimes developed.

Furthermore, the Horizon R-Q (Syn-rift II) interval in the Walvis Basin has a very distinctive facies. It thickens very rapidly both northwards and westwards, filling a trough related to the major east-west pre-Karoo fracture system that trended along the Walvis Ridge (Light et al., 1993). Low to moderate angle aggradational progradation is developed. Reflectors are mostly discontinuous and wavy, but some are more continuous. This sequence is interpreted to be a prograding deltaic unit where there was very rapid deposition of shales, silts and sands. Fluctuating shorelines probably gave rise to inter-bedded fluvial and aeolian clastics (Light et al., 1992, 1993). A zone of listric faulting developed in the west and the Syn-rift II sequence is not evident north of the Walvis Basin due to erosional truncation (Light et al., 1993).

2.2.4 Translational Megasequence

According to Light et al. (1993) the Transitional Megasequence marks the initial effects of thermal sag following the end of rifting and the first to contain signs of a developing shelf break. It is bounded below by Horizon Q (Hauterivian-Barremian), and above by Horizon P (Mid-Aptian). As the Atlantic Ocean continued to open, the rift basins transitioned into passive margin basins. The rifting ceased, and the extensional forces diminished. Sedimentary rocks began to accumulate in these basins, creating thick sequences of sedimentary strata (Ryberg et al., 2015). The Walvis Ridge, a submarine volcanic ridge, is a remnant of the earlier rifting phase.

Light et al. (1993) explained that most of the Q to P succession has been intersected in the Kudu wells west of the Medial Hinge Line, where it ranges from continental beds (basalts, and aeolian to fluvial sands) in the lower part, through shallow marine sandstones containing abundant carbonate cements, to shelly sandstones that locally grade into lagoonal shales, deeper marine siltstones and sapropelic shales at the top (Figure 4 and Figure *5*). The major Aptian marine transgression correlates with a global sea-level high stand.

The lower part of the megasequence above Megasequence SB2 is enigmatic (Mohammed et al., 2017). The recent studies by Mohammed et al. (2017) showed that this megasequence sits beneath a seaward dipping reflector package and has a thickness increase to the west across the margin but there is no evidence, at least in the current data, of significant faulting. The transitional phase comprises the transition from the syn-rift interval to the passive margin megasequences, which can be divided into a lower transition megasequence and an upper transition megasequence. The lower transition megasequence lies uncomfomably west of the basement high and is characterised by onlap or either the uppermost reflection of the syn-rift or on the basement/pre-rift ridge to the east.

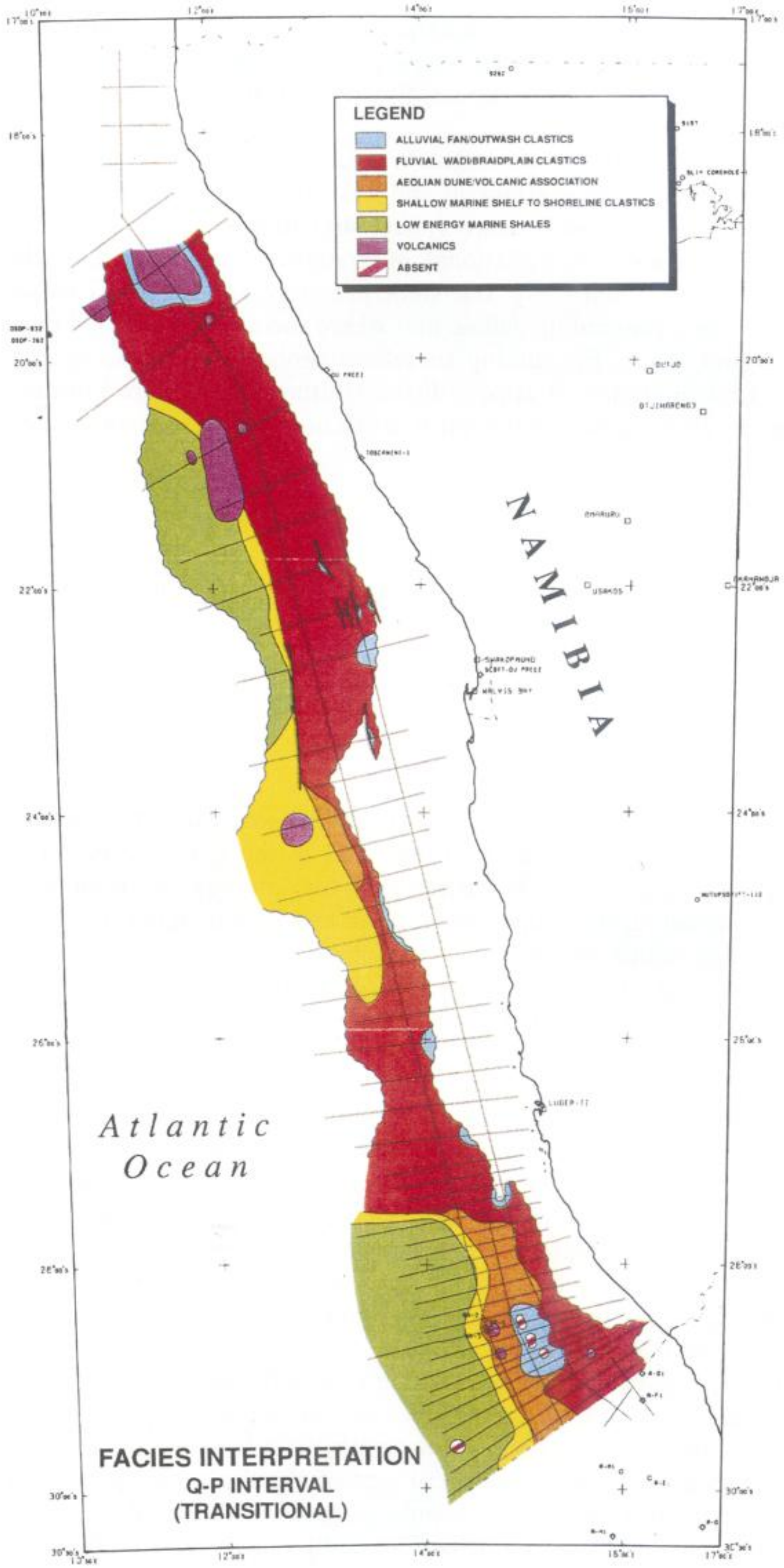
LEGEND
ALLUVIAL FAN/OUTWASH CLASTICS
FLUVIAL WADI/BRAIDPLAIN CLASTICS
AEOLIAN DUNE/VOLCANIC ASSOCIATION
SHALLOW MARINE SHELF TO SHORELINE CLASTICS
LOW ENERGY MARINE SHALES
VOLCANICS
ABSENT
NAMIBIA
Atlantic Ocean
FACIES INTERPRETATION
Q-P INTERVAL
(TRANSITIONAL)

Figure 5: Facies interpretation of the Transition interval which summarizes latest phase of rifting prior to the onset of thermal sag (Light et al., 1993).

2.2.5 Tertiary Thermal Sag Sequence

The earliest sequence associated with thermal sag along the margin is a progradational series that overlaps onto horizon P and is subsequently overlain by the Turonian unconformity N (see Figure 6). Horizon N marks a major transgression linked to the high global eustatic sea level around 95 million years ago (Light et al., 1993). Interpretations based on seismic velocity by Light et al (1993) the succession from N to the seafloor as consisting of open marine drift sediments. During the mid-Turonian (N) and the base Tertiary (L), a marine sequence was deposited. During the Late Cretaceous, there was a rapid progradation of the shelf resulting in a noticeable shelf break. This phenomenon led to the formation of intricate slump structures characterized by listric head scarp structures, basal detachment planes, and toe areas. The potential reservoir sandstone of Maastrichtian age in well 2012/13-1 may be linked to such gravity-driven turbidites

This Megasequence of Aptian and Turonian age developed during continued sagging and tilting of the continental margin offshore Namibia (Light et al., 1993). Light et al. (1993) further explained that it was characterized by a progradational succession that downlapped onto Horizon P. In the region of the Hinge Line, Horizon N was frequently truncated and displaced by a major Late Cretaceous/Tertiary listric slump detachment system that extends close to the level of Horizon P.

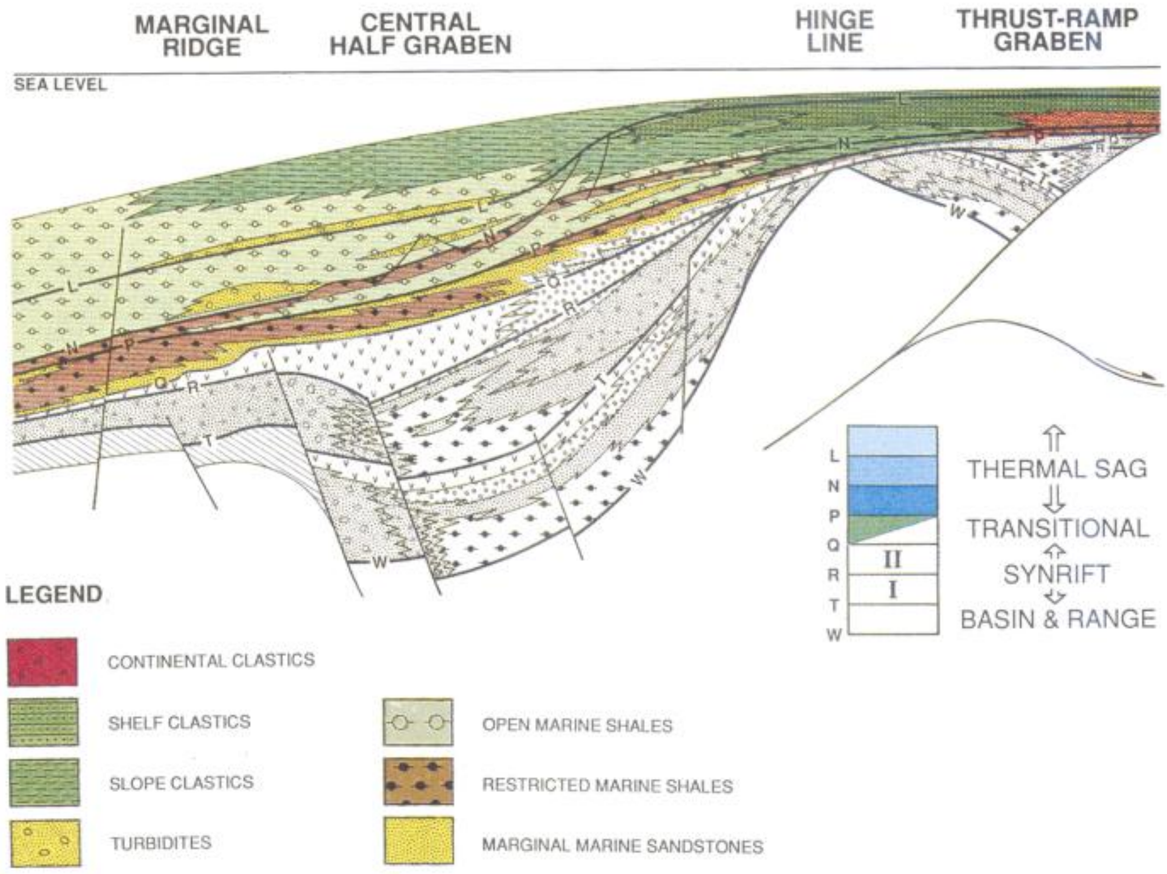

Figure 6: Thermal sag sequences (Light et al., 1993).

South of the Walvis Ridge is a major transgression began after Horizon N and the sea transgressed over the Hinge Line further to the east than in the preceding the Transitional Megasequence (Light et al., 1993). The distinct basins located south of the Walvis Ridge had formed a clearly defined east/west division comprising shelf, slope, and basin in the offshore Namibia region (Kukulus, 2004; Light et al., 1993). This period marks a progression of the marine transgression observed in the preceding transitional phase. On the shelf, seismic reflectors are essentially parallel, occasionally demonstrating indications of coastal onlap. In the eastern sector, these reflectors are more or less discontinuous or semi-continuous, with inter-bedded quieter zones, representing a succession of high-energy shoreline to shallow marine inner shelf sands, occasionally with inter-laminated shales and possibly thin layers of limestone (Kukulus, 2004; Light et al., 1993). Conversely, the western portion of the shelf is characterized by more continuous reflectors, again with quieter and transparent inter-beds, indicating the presence of lower-energy, outer shelf sands and shales situated beyond the reach of wave energy and coastal currents.

In the Namibe Basin the P-N (Aptian to Turonian) Megasequence is interpreted as a progradational build-out of the shelf edge, with some volcanicity occurring along the eastern flank of the continental basement ridge. On the Walvis Ridge, the volcanic dome was emplaced beneath by Horizon P and above by Horizon N indicating that it is of Aptian to Turonian (Light et al., 1993). Thick and extensive sets of prograding reflectors occur within the core of the volcano, probably representing rapidly deposited tuffaceous units which built-out to the west and north (Light et al., 1993).

2.3 Geology of the Walvis Basin

The Walvis Basin, located offshore northwest Namibia, is an area where sediment has been deposited from the Cretaceous period to Recent, approximately 105,000 square kilometers (Kukulus, 2004). It features a wedge-shaped structure characteristic of passive margin postrift sediments. Sedimentation begun to build out over an Early Cretaceous rift section until the Tertiary, constructing the basin system of the offshore area (Fernandes et al., 2003). Rifting and breakup of West Gondwana in the Late Jurassic and Early Cretaceous resulted in the formation of the South Atlantic Ocean.

The present Namibian Passive Continental Margin has undergone long-lived uplift and erosion characterised by the development of a major escarpment that generates two distinct drainage regimes (Kukulus, 2004). It is a as classical example of a volcanic margin (Clemson et al., 1997; Light et al., 1993). The offshore basins of Namibia and

South African western coast such as Orange, Lüderitz, Walvis and Namibe Basins from south to north were formed with the break-up of southwestern Gondwana and the opening of the South Atlantic Ocean (Fernandes et al., 2003; Light et al., 1993). The northernmost two are formed during the Walvis Ridge, and as a result the Namibe Basin has a closer affinity with the Angolan Shelf than with the basins further south (Light et al., 1993).

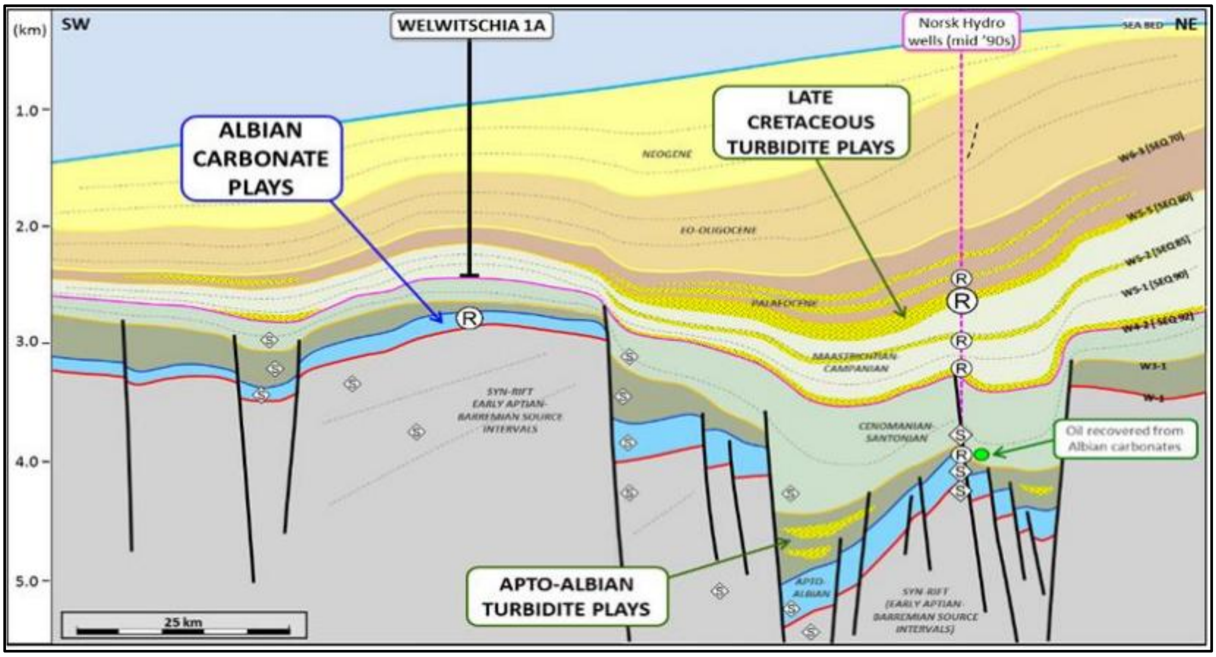

Figure 7: Geological cross-section through the Walvis Basin (Tower, 2020).

Basin & Range rifting was initiated in the southern region and moved northward towards the Walvis Ridge. This progression persisted through subsequent rift events. Initially, the impact was felt in the southern offshore area during the first syn-rift phase (Syn-rift I). However, the second syn-rift phase (Syn-rift II) extended further north, thickening within the Walvis Basin (see Figure 7 and Figure 8).

The primary faults in the basins, such as the Walvis Basin, situated south of the Walvis Ridge, dip towards the land. Conversely, north of the ridge, seismic imaging off the coast of Namibia reveals faults (normal and listric faults) dipping seaward, known as seaward dipping faults (Figure 7 and Figure 8).

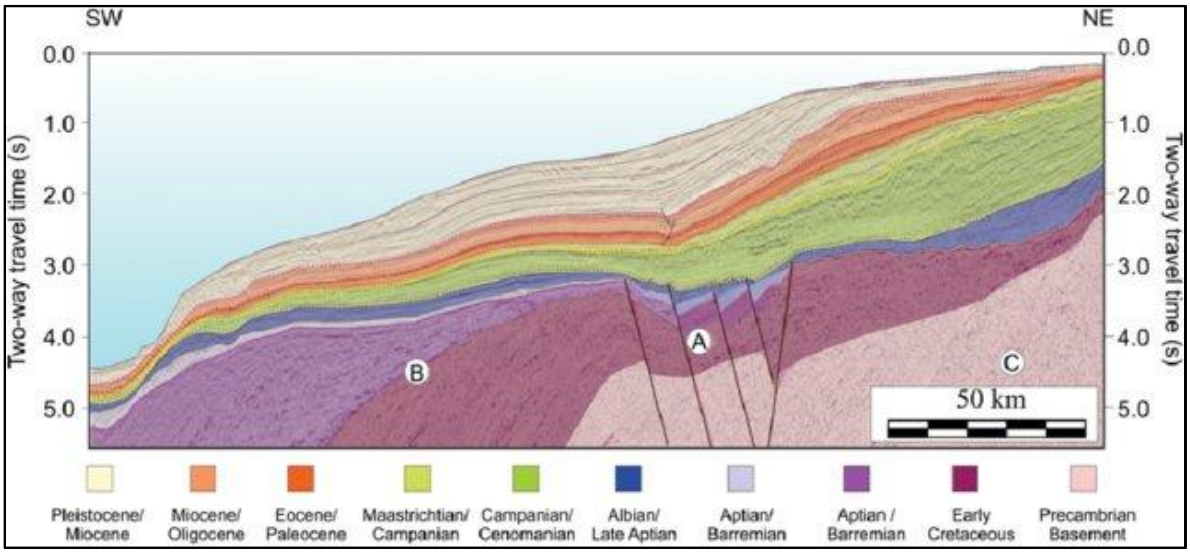

Figure 8: The regional seismic profile in the Walvis Basin offshore Namibia illustrates the shift from continental to oceanic crust through extensive layers of SDRs (syn-rift deposits)., A shows continental basement intruded during the Barremian-Aptian rifting, B denotes a wedge of SDRs and C represents continental crust (Blaich et al., 2013)

The Walvis Basin exhibits the characteristic wedge-shaped configuration typical of post-rift formations, resembling the geometry of a passive margin, with water depths ranging from 150 to 3000 meters. It remains largely unexplored, yet recent drilling findings, as indicated by Bray et al (1998), suggest promising elements for a viable petroleum system.

2.4 Comparing Walvis Basin with other neighboring Basins

The Walvis Basin offshore NW-Namibia is a Cretaceous to Recent depositional centre that covers an area of 105000km^2 (Kukulus, 2004). It is a typical post-rift wedge shaped, with geometry of post rift passive margin (see Figure 10- Figure 11).

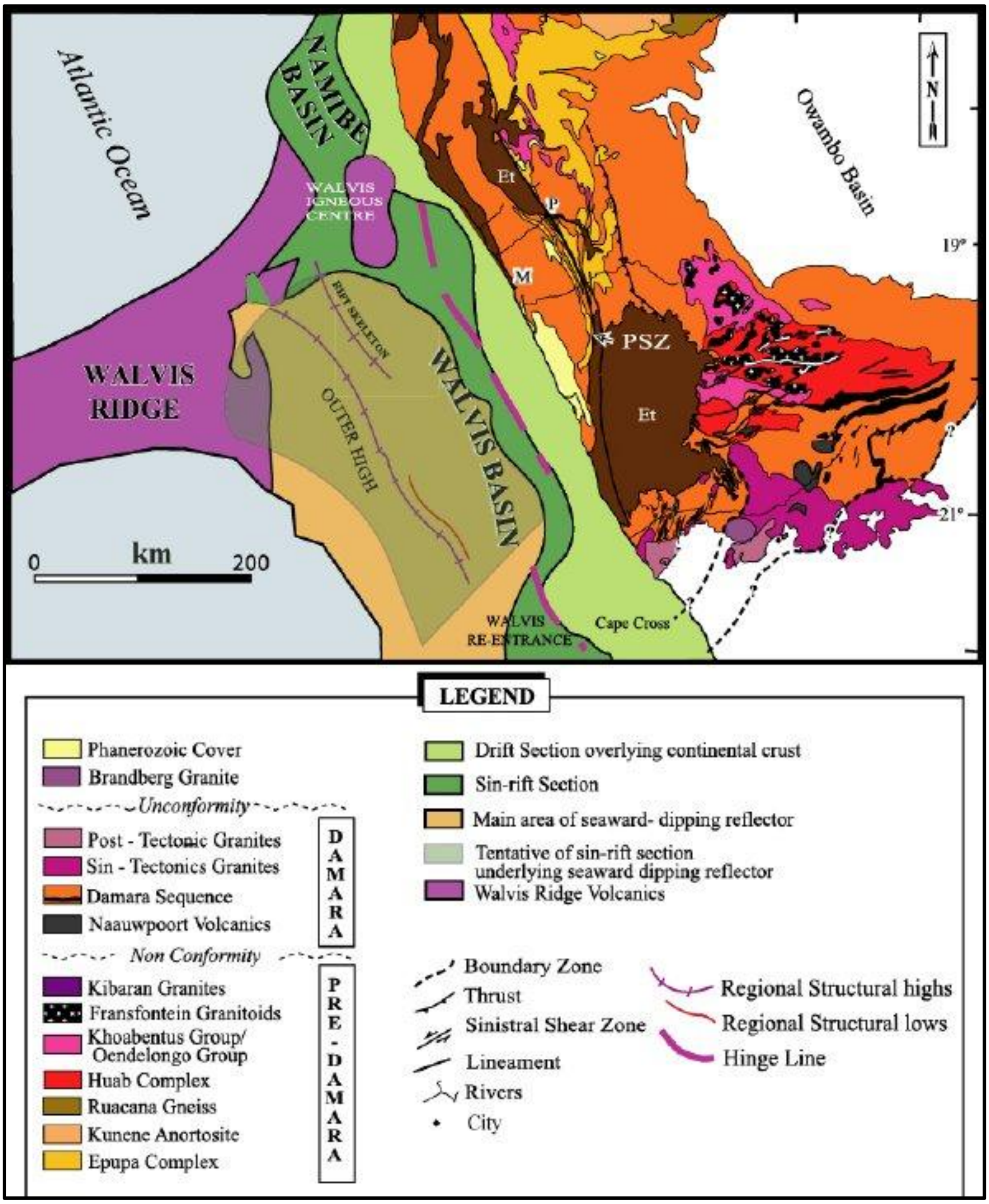

Figure 9: Geological map of the NW Margin of Namibia showing the Walvis Basin and its adjacent basement (Kaoko Belt and Congo Craton) (Fernandes et al., 2003).

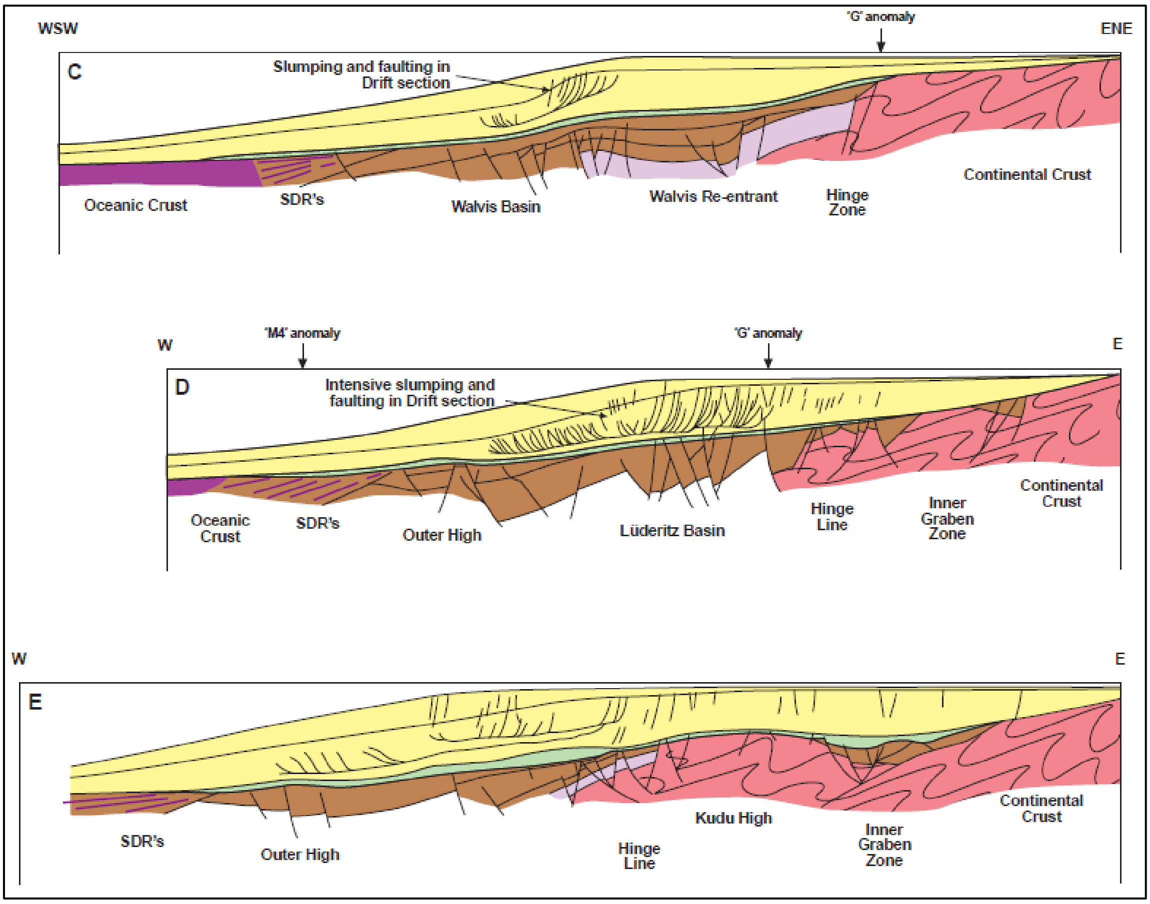

Figure 10: The Structural framework of the southern basins. The upper part illustrates the Walvis Basin, the middle portion represents the Lüderitz Basin, and the lower part which is corresponds to the Orange Basin. The Walvis Basin is a typical post-rift wedge shaped, with geometry of post rift passive margin, distinguishing it from the other two basins (Bray et al., 1998).

The underexplored offshore deepwater basins of Angola and Namibia hold tremendous potential for hydrocarbons. Walvis Basin is one of the four offshore hydrocarbon basins of Namibia. Namibia has four offshore basins, namely, the Orange Basin, South of Namibia, bordering South Africa; the Lüderitz Basin, the Walvis Basin and Namibe Basin. These basins were formed during the Late Jurassic to Early Cretaceous breakup of Gondwana (Blaich et al., 2011).

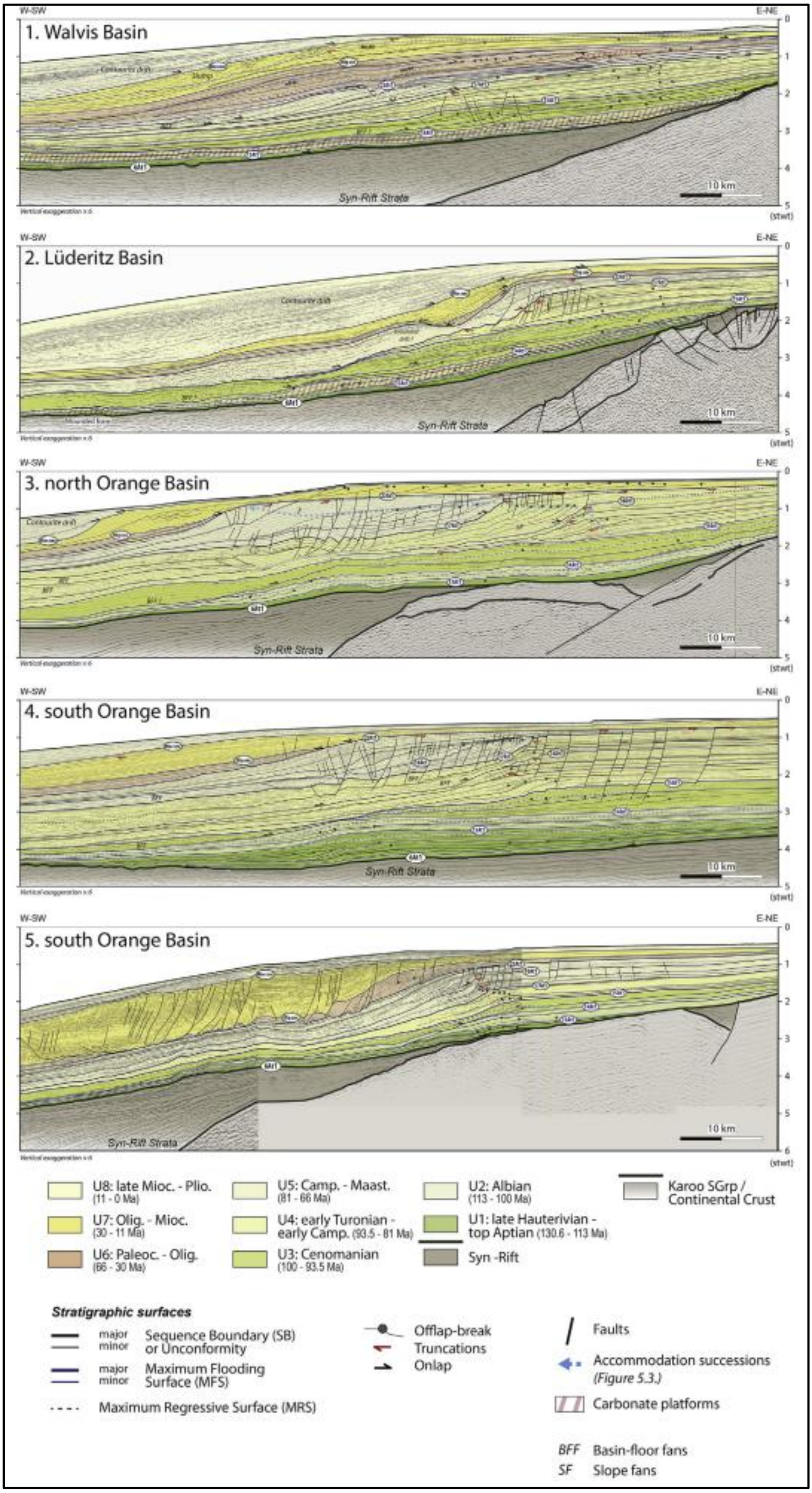
W-SW
E-NE
1. Walvis Basin
Syn-Rift Strata
10 km
(stwt)
2. Lüderitz Basin
Syn-Rift Strata
10 km
3. north Orange Basin
Syn-Rift Strata
10 km
4. south Orange Basin
Syn-Rift Strata
10 km
5. south Orange Basin
Syn-Rift Strata
10 km
U8: late Mioc. - Plio. (11 - 0 Ma)
U7: Olig. - Mioc. (30 - 11 Ma)
U6: Paleoc. - Olig. (66 - 30 Ma)
U5: Camp. - Maast. (81 - 66 Ma)
U4: early Turonian - early Camp. (93.5 - 81 Ma)
U3: Cenomanian (100 - 93.5 Ma)
U2: Albian (113 - 100 Ma)
U1: late Hauterivian - top Aptian (130.6 - 113 Ma)
Syn -Rift
Karoo SGrp / Continental Crust
Stratigraphic surfaces
major minor Sequence Boundary (SB) or Unconformity
major minor Maximum Flooding Surface (MFS)
Maximum Regressive Surface (MRS)
Offlap-break
Truncations
Onlap
Faults
Accommodation successions (Figure 5.3.)
Carbonate platforms
BFF Basin-floor fans
SF Slope fans

Figure 11: Illustrations of five seismic profiles capturing the primary depocenters along the Atlantic Margin of Namibia and South Africa (Baby et al., 2018)

Recently acquired broadband 2D seismic from the Namibe Basin (offshore Angola) and offshore Namibia has allowed a detailed imaging of syn-rift and post-rift structures, enabling identification and mapping of prospects analogous to those so prolific in the South American conjugate margins (Baby et al., 2018).

According to Kukulus (2004) three potential intervals of reservoir rock were developed within the early to late drift sequence. Detailed analysis of samples from Upper Campanian/Maastrichtian fan sands allowed thorough characterization of reservoir quality. While the main sand body with a porosity of up to 21%, and net – to – gross of 0.3. Notably, the presence of clay minerals is negligible; however, the limitation on permeability stems from intense late-stage cementation by dolomite. Despite the lack of confirmation of the predicted structural and stratigraphic closure for the Maastrichtian reservoir by well 2012/13-1, it is apparent that hydrocarbons have migrated.

Although hydrocarbons from reservoirs appear to be absent, essential components of a viable hydrocarbon system are present in the central and northern Walvis Basin. This suggests that further assessment and exploration efforts are warranted.

2.5 Hydrocarbon Potential in offshore, Namibia

The Aptian source rock has been observed in the discovery well of the Kudu field. This Aptian source rock is believed to be deposited in a restricted marine environment which is both oil and gas prone (Bray et al., 1998). The Aptian source rock measures is about 140 meters thick overlying thinner source rock intervals of the Barremian period. It has an average Total Organic Carbon (TOC) content of approximately 2% (Bray et al., 1998).

The subsequent younger source rock from the Cenomanian to Turonian appears to be absent in the Kudu Field. However, this source rock correlated with a stratigraphic equivalent oil-prone source rock found in the Orange Basin. Moreover, there is a promising Cretaceous-age marine source rock with good oil-producing potential identified in the Walvis Basin. The Cenomanian-Turonian source rock has an average TOC of 5%, and even though the shales are not yet thermally mature, there's potential for hydrocarbon generation given sufficient burial depth (Bray et al., 1998).

The syn-rift interval may also be a potential source rock. It is believed that during the initial stages of rifting, lacustrine environments formed, which could have preserved organic rich oil-prone claystones. In the South African Orange Basin, oil-prone lacustrine source rocks are expected to be found in the Hauterivian syn-rift section (Hartwig, 2014). Proven reservoirs include the pre-rift sandstones and carbonates, syn-rift continental sandstones, Aptian carbonate and late Cretaceous/Tertiary turbidites. These reservoirs have been identified in Well 1911/15-1 in the Walvis Basin, with porosity ranging from 15% to 31%. Specifically, the Campanian-Maastrichtian deep marine turbidites in the mentioned well has a porosity of 16-25%, while the deep marine fans very good porosity ranging from 26% to 31% (NAMCOR E&P, 2016).

The Kudu Field has demonstrated the presence of Early Cretaceous transitional reservoirs. These reservoirs consist of aeolian sandstones intercalated with volcaniclastic deposits, marine sandstones, and shaley limestones. With an average net thickness of 50 meters and porosity reaching up to 20%, they hold significant potential for extraction (NAMCOR E&P, 2016). Additionally, there are prospective deep-water reservoirs in the form of basin floor fans located above the mid-Aptian and upper Santonian unconformities in the deeper northern section of Kudu Field. Furthermore, marginal marine and fluvial sand deposits within the syn-rift section also contribute to the reservoir potential (Spectrum, 2012).

Similarly the Orange Basin, the Lüderitz Basin also holds potential reservoirs spanning the Lower Cretaceous, Upper Cretaceous, and likely into the Palaeogene periods. A thick layer of shallow marine shelf sand has been identified in well 2513/8-1, 1363 to 1408 meters deep, with an average porosity of 17%. Mesozoic intra-formational shale, occurring at various depths, has been identified as potential cap rock in the Walvis Basin. Additionally, in the Orange Basin, the Barremian and Aptian source rocks also act as seal rocks (NAMCOR E&P, 2016).

Onshore, there are two extensive Neoproterozoic or Early Cambrian Basins: the Owambo Basin in the north and the Nama Basin in the south (NAMCOR E&P, 2016). Most onshore exploration and stratigraphic wells are relatively shallow and have not fully explored. Nonetheless, both offshore and onshore exploration efforts have confirmed there is a functioning petroleum system, comprising multiple reservoirs, source rock, trap, and seal sequences.

2.6 Seismic sequence stratigraphy analysis

Seismic stratigraphy is used at the exploration level, while sequence stratigraphy, based on chronostratigraphy principles, is employed at the production level (Al-Masgari et al., 2021). This approach utilizes Vail's concepts in relation to cores, wireline logs, and outcrops. Seismic sequence stratigraphy may also be used to analyze seismic sequences and depositional time units by identifying unconformities or changes in seismic patterns (Vail, 1987). On the other hand, seismic facies focuses on defining depositional environments by analyzing the characteristics of seismic reflection data.

Seismic-stratigraphic data offer comprehensive insights into seismic prospects by defining structural features, stratigraphy, and lithology (Taner et al., 1979; Van Wagoner et al., 1990). For instance, seismic analysis has been used to characterize trapping systems within the Kribi-Campo sub-basin (Le, 2012). Seismic stratigraphy examines geological stratigraphy by identifying patterns in seismic reflections that may indicate various types of stratal terminations, such as onlaps, downlaps, erosional truncations, and toplaps. A study by (Kabaca, 2018) demonstrated an approach for semi-automatically identifying sequence-bounding surfaces using seismic waveform, acoustic impedance, and porosity attributes to evaluate source rocks, reservoir rocks, and seal rocks in petroleum system analysis within a basin.

Chongwain et al. (2021) identified various sequences by picking three main horizons for their seismic interpretation. The reservoirs and deeper sands exhibit lateral variations in seismic response, which relate to changes in reservoir properties and the presence of hydrocarbons. Seismic data reveals sedimentary features like channels and pinch-outs, which likely serve as stratigraphic traps to the east. All major faults were identified and seven facies units in the Douala Basin, Cameroon, through seismic analysis. Joseph (2020) predicted lithofacies in the Lüderitz Basin using seismic stratigraphic interpretation, revealing several source, seals and reservoir rocks. The mapping of seismic marker horizons was carried out using Petrel software which identified the likely main source rock intervals, as well as stratigraphic surfaces such as unconformities, downlap surfaces, and onlap surfaces. Seismic facies mapping was then carried out within stratigraphic packages defined by these previously identified horizons. Lithofacies were identified based on seismic facies, system tracts, and analogue interpretations. The seismic attributes of 2D seismic data in the offshore Cenozoic of the Kribi-Campo sub-basin were analyzed to understand the seismic stratigraphic distribution, the evolution of paleoenvironments, and to evaluate the hydrocarbon potential of the Cenozoic offshore deposits (Yugyè et al., 2022). Five seismic facies such as parallel to subparallel, hummocky, chaotic, sigmoidal, and oblique were identified and seismic stratigraphic unit was sub-divided into five major unconformities dated Upper Paleocene, Lower Eocene, Middle Miocene, Upper Miocene, and Pliocene to Pleistocene. The potential for oil and gas exploration in the offshore Cenozoic sub-basin was emphasized based on the presence of potential source rocks, reservoirs, seals, structural and stratigraphic traps across the studied seismic intervals (Yugyè et al., 2022).

CHAPTER 3: MATERIALS AND METHODS

3.1 Introduction

The hydrocarbon exploration dataset was made available through the National Petroleum Corporation of Namibia (NAMCOR). This chapter present seismic data, well reports, and presentations created the database upon which seismic stratigraphic analysis for the characterisation of petroleum system elements studies carried out using the flowchart in Figure 13.

3.2 Data

3.2.1 Seismic data

Selected lines of the VERNWB-03, ION GXT, NWG-98, PGS MC2D, TGS-11, ECL-91, and N2R-93 seismic datasets on blocks 2011B and 2111A (Figure 2 and Figure 12) were used for this study. 2D seismic dataset on blocks 2011B and 2111A were used for this study.

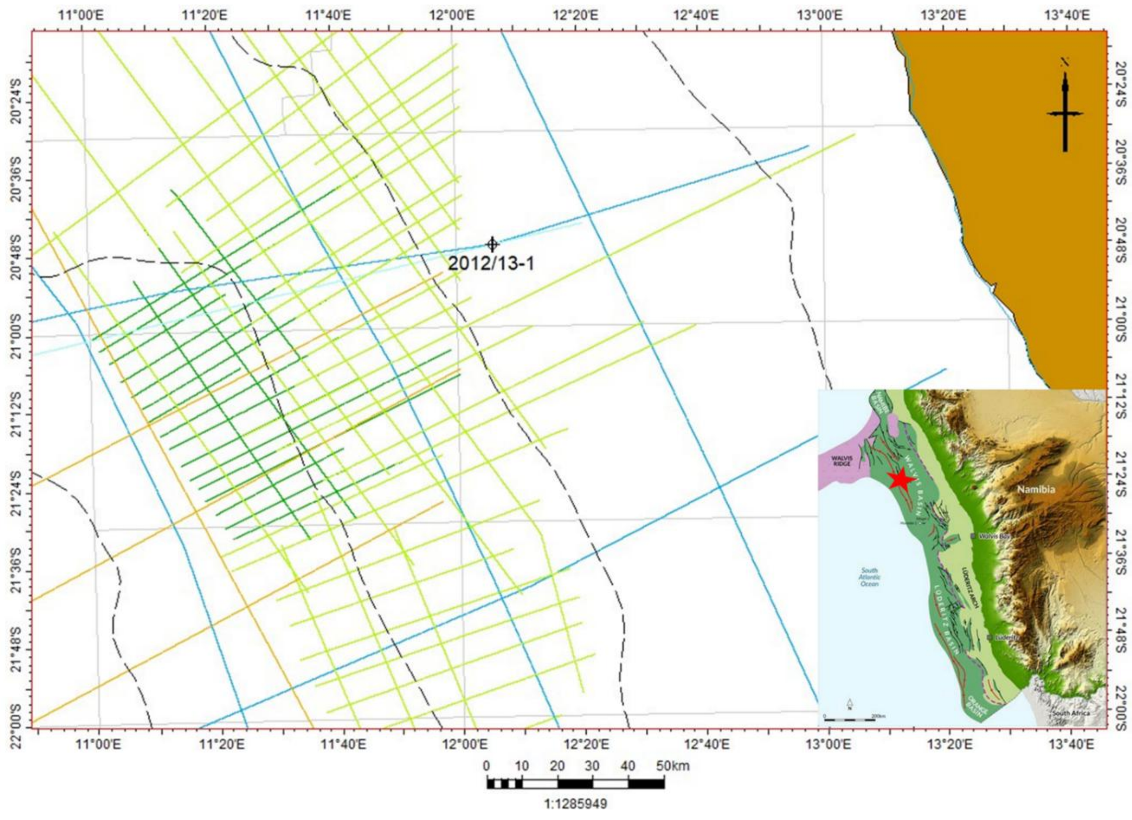

Figure 12: Location of the study area, Walvis Basin Selected lines of the VERNWB-03, ION GXT, NWG-98, PGS MC2D, TGS-11, ECL-91, and N2R-93 seismic datasets [Modified: https://www.ecooilandgas.com/projects/namibia/]

3.2.2 Well data

Wells enable the study of subsurface stratigraphy using cores and logs at single or multiple locations. The exploration wells in the Walvis Basin are well 2012/13-1 (Figure 12) for which the final well report as well as the Sasol biostratigraphy report was accessible. The final well report contains information on drilling parameters, lithologies and a brief geological evaluation. The Cormorant-1 and 2012/13-1 well biostratigraphy reports were used for the study. Within this interval a sequence stratigraphic interpretation and an estimate of paleo water depth is 627.7 meters.

Furthermore, biostratigraphic data for well 2012/13-1 was utilized to examine significant stratigraphic features, such as maximum flooding surfaces and sequence boundaries. These features are characterized by the abundance and diversity of specific nannofossils, palynofloras, and micropaleontological assemblages (Sasol Petroleum [Namibia] Pty Ltd., 1997). In well logs, these surfaces are distinguished by high gamma-ray counts, accompanied by a sharp drop in spontaneous potential (SP) log close to zero (Sasol Petroleum [Namibia] Pty Ltd., 1997). Additionally, the combination of resistivity and gamma-ray logs has been employed to discern depositional settings in the subsurface, allowing for the identification of texture trends (shale-sand) and the deduction of stratal stacking patterns (Sasol Petroleum [Namibia] Pty Ltd., 1997).

3.3 Procedures

3.3.1 Seismic sequence analysis

Seismic sequence analysis was applied to identify depositional sequences and systems tracks on seismic sections by interpreting the location of their boundaries. Seismic sequence analysis was carried out on the seismic data by picking major unconformities identified from reflector terminations, change in seismic facies character, or choosing significant boundaries from well data using approach described in Futalan et al. (2012) and Joseph (2020).

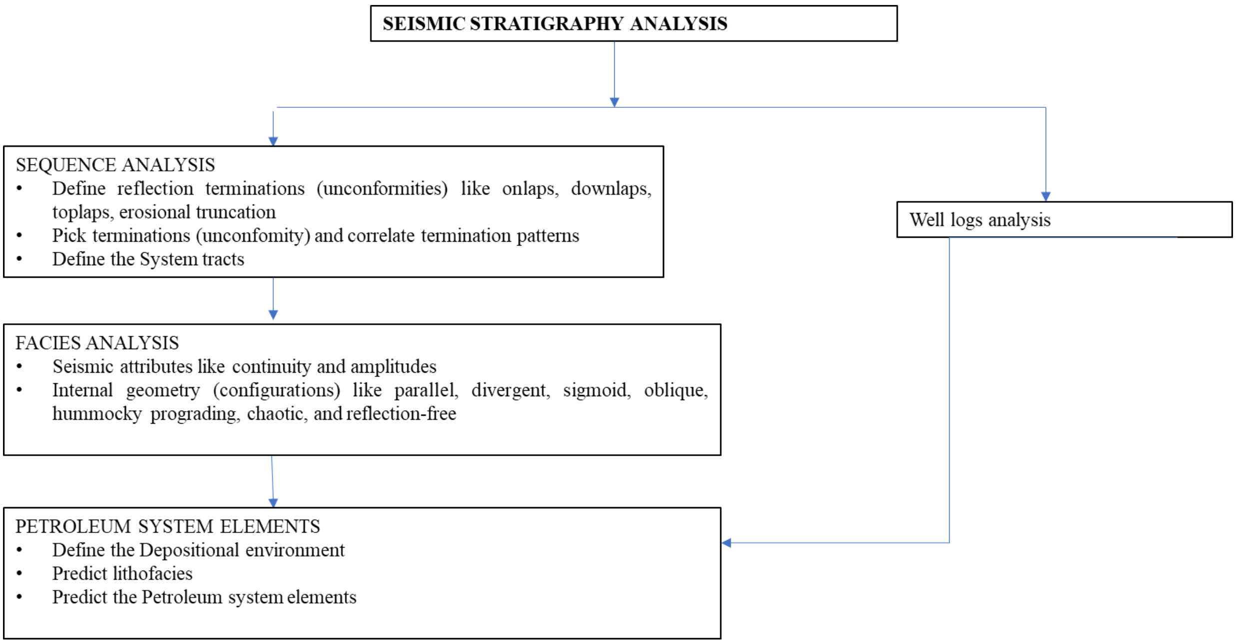

Figure 13: Seismic stratigraphy modeling flow chart

3.3.1.1 Major horizon

Strong seismic reflectors were picked as they serve as marker horizons, often of stratigraphic significance. Seismic horizons were mapped manually and using Petrel 2022 software. Mapping of seismic marker horizons included the identification of main source rock intervals, stratigraphic surfaces such as unconformities, downlap surfaces, and onlap surfaces. Seismic facies mapping was carried out within stratigraphic packages that are bounded by the previously identified stratigraphic horizons.

3.3.1.2 Identification of Seismic Stratigraphic Surfaces

The key stratigraphic surfaces i.e. Sequence Boundary (SB), Transgressive Surface (TS) and Maximum Flooding Surface (MFS) (see Figure 14) were interpreted separately in wireline log data and seismic following the procedure outlined in the studies by Mitchum Jr et al. (1977) and Parvin and Woobaidullah (2019) studies. .

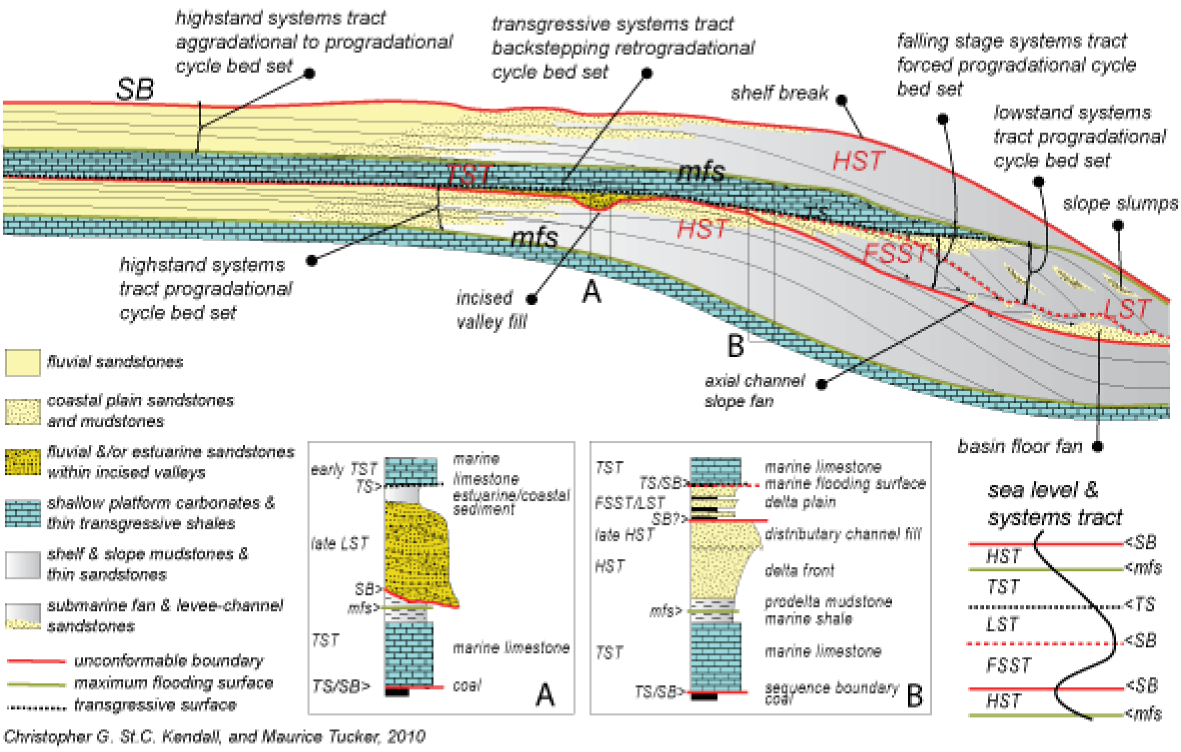

Figure 14: Parasequence sets and system tracts (Mitchum Jr et al., 1977)

In the Well Log, Sequence Boundary (SB) was placed at the coarsening upward log shape comprising Lowstand System Tract (LST) till the overlying Transgressive Surface (TS) whereas TS was placed at the base of fining upward log shape followed by the LST (see Figure 14) (Parvin & Woobaidullah, 2019). This log pattern develops

TST till the Maximum Flooding Surface (MFS). MFS picked at the maximum shale value or maximum gamma ray value. In the seismic, Sequence Boundary (SB) was interpreted from onlap, truncation relation whereas Maximum Flooding Surface (MFS) was interpreted from downlap. TS on seismic was drawn at the Transgressive Surface (TS) point on well after seismic to well tie. Finally, both interpretations (well and seismic) were tied up using Petrel 2022 software to obtain fieldwide stratigraphic configuration of the stratigraphic surfaces. Then, the gamma ray (GR), spontaneous potential (SP), resistivity log (LLD), and density (PHID) logs were used to categorize the lithology of the prospective zones.

3.3.1.3 Reflection Termination Mapping

Reflection terminations were mapped following the procedure given in or outlined by (Al-Masgari et al., 2006; Joseph, 2020) for seismic section sequence analysis. The following steps were executed:

- The places where the two reflectors converge were attained (there are always terminations where reflectors converge).
- The reflector terminations were marked with arrows.
- The discontinuity surface between the onlapping and downlapping reflections was drawn below the reflector termination, and the truncating and toplapping reflectors above the reflector terminations. The position of the discontinuity surface where it becomes conformable was traced across the section using reflection correlation (Figure 15).

Each discontinuity was categorised according to the classification described in (Vail, 1987). A discontinuity demonstrating a regional downlap above and truncation below was interpreted as the upper sequence boundary. Toplap refers to the termination of strata against an overlying surface due to non-deposition or minor erosion, while truncation implies deposition of strata followed by tilting and removal along an unconformity surface. Such termination serves as a reliable top-discordant criterion for a sequence boundary and can also result from termination against an erosional surface, such as a channel.

A discontinuity demonstrating a regional downlap, was interpreted as a downlap surface marking the lower sequence boundary. Onlap involves horizontal strata progressively terminating against an initially inclined surface or in which initially inclined strata terminate progressively updip against a surface of greater initial inclination, while downlap entails seismic reflections of inclined strata terminating downdip against an inclined or horizontal surface (Figure 15). Examples of downlap surfaces include top basin floor fan surface, top slope fan surface, and maximum flooding surface.

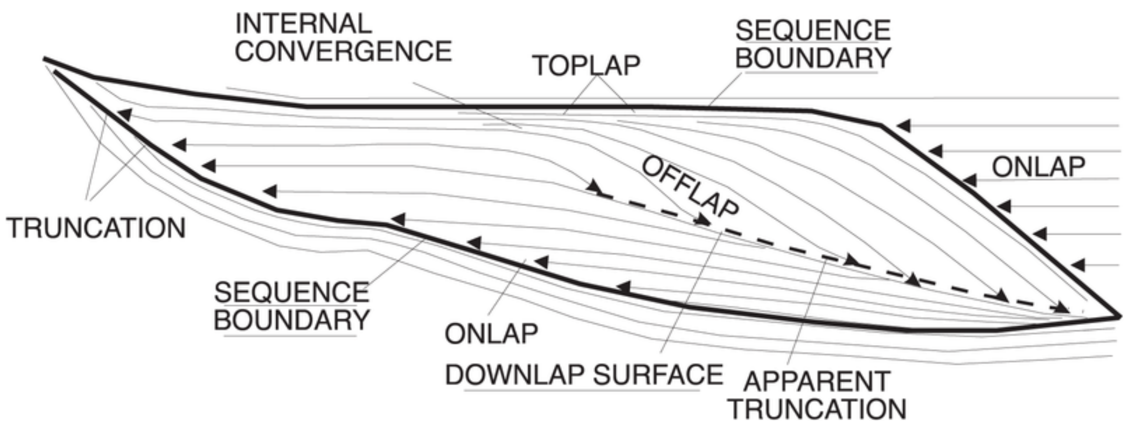

Figure 15: Reflection termination patterns which shows relatively conformable succession of genetically related strata (Vail, 1987)

3.3.1.4 System Tracts

Sequences were subdivided into systems tracts by considering various factors such as the nature of bounding surfaces, their placement within a sequence, stacking patterns of parasequences, geometric characteristics, and associations with specific facies (Van Wagoner et al., 1990). The stratigraphic succession showed four distinct system tracts, developed under the effect of changes in base level and sediment supply (Mitchum Jr et al., 1977; Wu et al., 2019). The first is the Lowstand System Tract (LST) (see Figure 16 and Figure 16), extending from the lowest point of sea level to the furthest regression point during a phase of rising relative sea levels. Next is the Transgressive System Tract, spanning from the maximum regression to the peak transgression in the context of rising relative sea levels. The third tract is the Highstand System Tract, encompassing the period from maximum transgression to the subsequent drop in relative sea level during a rise. Finally, the Forced Regressive System Tract covers the entire duration of a relative sea-level decline, extending from the onset to its conclusion.

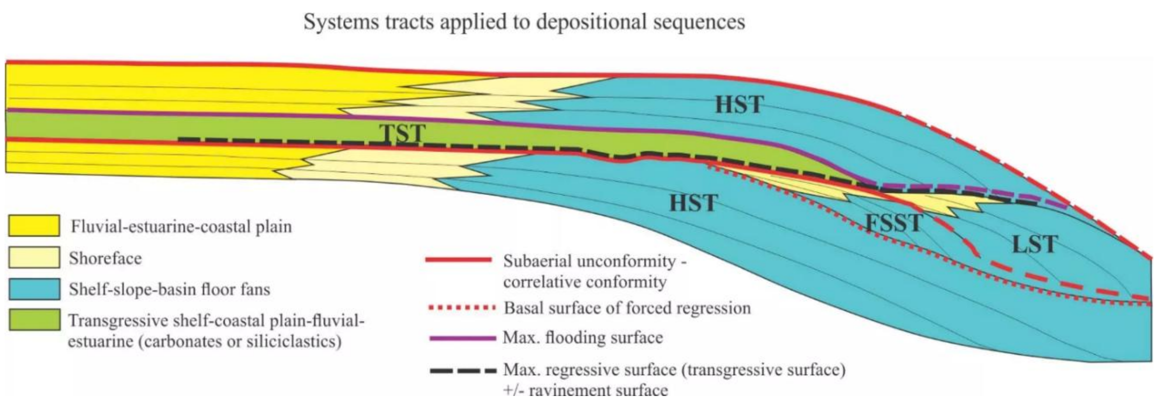

Figure 16: Two-dimensional, dip-parallel profile showing the systems tract configuration for the standard depositional sequence model. Systems tracts are: TST transgressive; HST highstand; FSST falling stage; LST lowstand; RST regressive.

Derived from https://www.geological-digressions.com/depositional-systems-and-systems-tracts/

In this research, the lowstand systems tract (LST), transgressive systems tract (TST), and highstand systems tract (HST) are used to divide sequences (see Figure 16). The lowstand systems tract was formed when there is a substantial decline in sea level, leading to extensive subaerial exposure and/or widespread fluvial incision (manifested as thick paleosol and/or incised valleys, respectively). These lowstand systems tracts are delineated by a sequence boundary and the initial significant marine flooding surface (FS). Transgressive systems tracts are bounded at the base by the first major marine flooding surface, and at the top by the maximum flooding surface (MFS). The maximum flooding surfaces serve as indicators for the widespread formation of a compacted section primarily composed of hemipelagic or pelagic sediments. In this study, the identification of maximum flooding surfaces is based on selecting points with the highest gamma-ray values within a given sequence (API). The consistent presence of the highest gamma-ray values serves as a reliable marker and seems to be associated with the development of a condensed section during the peak of flooding. As for the highstand systems tract is bounded at the base by the maximum flooding surface and at the top by the overlying sequence boundary.

3.3.2 Seismic facies analysis

Seismic facies are mappable three-dimensional seismic units that are composed of group of reflections whose parameters differ from those of adjacent facies units. Seismic facies analysis involved interpreting both the environmental conditions and lithofacies based on seismic data. Various seismic facies types were systematically identified based on the main reflector characteristics including reflector geometry, reflector continuity, reflector amplitude and reflector frequency (see Table 3)

(Mitchum Jr et al., 1977). Each seismic facies identified was assigned a unique two-way time which was mapped in the seismic grid in creating the distribution framework of the seismic facies and in generating facies maps. Once these units were identified, their boundaries were delineated, and their spatial relationships were mapped out. Subsequently, they were analyzed to reveal insights into the stratification, lithology, and depositional features of the formations responsible for generating the reflections within these units.

For this study, depositional sequences were divided into seismic facies units on all seismic sections. The internal reflection configuration and terminations of each seismic facies unit, i.e., sigmoid, parallel, downlap.

The seismic facies from a grid of sections (vertical) of 2-D seismic data was analysed according to Mitchum Jr et al. (1977). Each depositional sequence was divided into seismic facies units on all seismic sections. The following steps were done.

- The internal reflection configuration and terminations of each seismic facies unit, i.e., sigmoid, parallel, downlap was analysed as in Table 2. Different types of reflection configurations were observed, including parallel, subparallel, divergent, prograding, chaotic, and reflection-free areas. Prograding configurations was further categorized into sigmoid, oblique, complex sigmoid-oblique, shingled, and hummocky clinoform configurations as in Table 2.
- The combination of seismic facies distribution and thickness distribution of any other diagnostic parameters, like interval velocity or localized amplitude anomalies, was executed.

- The incorporation of well and outcrop data into the seismic facies distribution was undertaken.
- The lithology was estimated using depositional setting interpretation. The interpretation of seismic facies maps entailed considerations of various depositional settings, such as marine or nonmarine environments, water depth, basin position, energy, transport direction, and other pertinent depositional factors as shown in Table 2 and Table 3. External forms of seismic facies units were reported to include sheet, sheet drape, wedge, bank, lens, mound, and fill forms. Seismic facies units were interpreted in terms of the depositional environments, the energy of the depositing medium, and the potential lithologic content of the strata generating the seismic facies reflection pattern.

Table 2: Reflection parameters for evaluation and interpretation of seismic facies (Mitchum Jr et al., 1977)

Seismic facies	Reflection configuration	Reflection continuity	Reflection amplitude and frequency	Bounding relationship	Depositional environment interpretation	Example (Vertical scale bars represent 100 ms)
1 Parallel continuous high amplitudes	Parallel	Continuous	High amplitude and low frequency	Continuous and draping underlying topography	Pelagic or hemipelagic	
2 Semiparallel continuous high amplitudes	Semiparallel	Continuous to semicontinuous	High amplitude and high frequency	Restricted to the top of the regional anticline	Debris flows or hyperconcentrated density flows or turbidites	
3 Mounded discontinuous low amplitudes	Contorted to mound-shaped	Discontinuous	Low amplitude and high frequency	Onlap, downlap, toplap, and truncation	Debris flows or (hyper) concentrated density flows	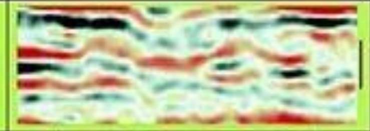
4 Blocky semicontinuous high amplitudes	Oblique	Semicontinuous	High amplitude and high frequency	Separated by linear vertical to oblique surfaces	Lower slope and slumps or large lithified collapse blocks	
5 Oblique semicontinuous high amplitudes	Oblique	Semicontinuous	High amplitudes	Thinning out toward the platform	Upper slope	
6 Chaotic amplitudes	Chaotic	Discontinuous	Low amplitude	Grading vertically to facies 7 and laterally to facies 5	Platform interior	
7 Mounded semicontinous high amplitudes	Contorted to mound-shaped	Semicontinuous	High amplitude and low frequency	Numerous diffraction hyperbolas	Karstified platform top	

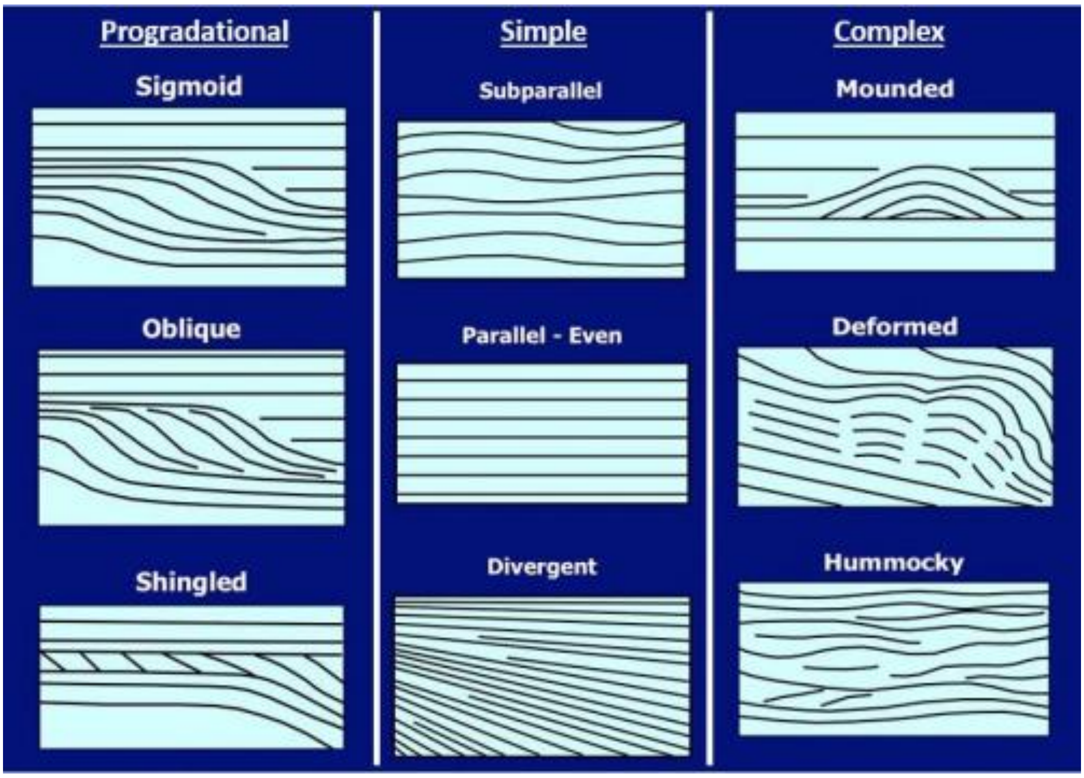

Figure 17: Typical seismic reflection patterns illustrating the concept of seismic facies (Mitchum Jr et al., 1977).

Table 3: Reflection parameters for evaluation and interpretation of seismic facies (Reflection parameters and their geological interpretation) modified from (Mitchum Jr et al., 1977)

	Seismic Characteristics
Reflection Parameter	**Geologic interpretation**
Configuration	• Bedding patterns • Depositional properties • Erosion and paleotopography • Fluid contacts
Continuity	• Lateral continuity of strata • Depositional processes
Amplitude	• Velocity and density contrasts of individual interfaces • Bed spacing • Bed thickness
Frequency	• Bed thickness • Fluid content
Internal velocity	• Lithofacies estimation • Porosity estimation • Fluid content

3.3.3 Identification of the Major Petroleum System Elements (source, reservoir, traps etc)

3.3.3.1 Identification of lithofacies

Once the objective aspects of delineating seismic sequences and facies were completed, the final objective was to interpret the facies in terms of lithofacies and depositional environments. The most useful seismic parameters in the seismic facies analysis were the geometry of reflections (reflection amplitude, continuity, frequency) and reflection terminations (onlap, downlap, erosional truncation, toplap); reflection configuration (parallel, divergent, sigmoid, or oblique) and three-dimensional form.

Lithofacies were identified on seismic data. This was done by relating possible lithofacies to the seismic facies. Each seismic facies type identified was correlated with well data biostratigraphy reports from Walvis Basin wells to establish a relationship between the seismic facies and lithofacies. Correlation panels were generated to illustrate the lithofacies that correspond with each seismic facies. A gross lithologic map was generated for each interval after establishing the relationship between the facies.

3.3.3.2 Identification of the major petroleum system elements

Lithofacies were selected for the model based on well and seismic data regarding stratigraphy and depositional interpretations. Well data revealed a diverse array of lithofacies across the basin.

The source rocks, reservoir rocks and seal rocks lithologies were delineated based to the lithofacies model in Table 2.

CHAPTER 4: RESULTS AND ANALYSIS

The results of this study are presented in Figure 18 to Figure 24.

4.1. Seismic stratigraphic intervals and horizons

A total of sixteen stratigraphic intervals were identified on the seismic section, between top basement and the seabed (Figure 18). The characteristics of each dividing stratigraphic surface, such as sequence boundaries, are also described in this chapter. Seismic reflectors, which depict chronological timelines were arranged by age and delineated with consistent time intervals for each horizon. A total of 14 Seismic Intervals (SI) were recognized.

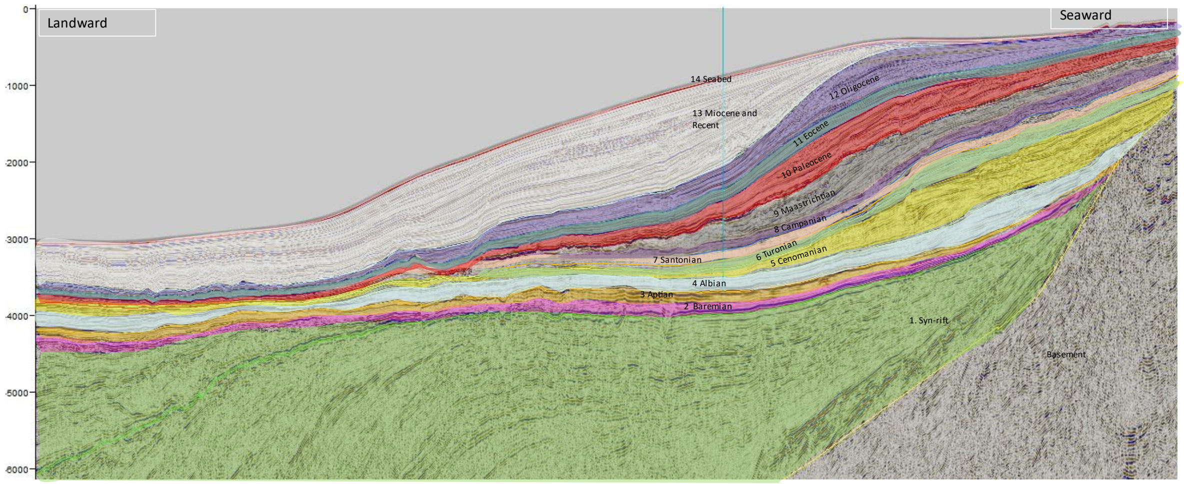

Figure 18: Dip line ION-GXT NAM -3000_pstm_stk_20150710 is annotated with seismic intervals and their corresponding ages which were obtained from well 2012/13-1 reports.

Lithofacies have been deduced by considering seismic facies, distance from the continent, and the mechanism of sediment transport. This analysis was supplemented by studying analogous sections of the Namibian margin.

4.1.1 Syn-rift Megasequence

The seismic interval SI 1 represents a syn-rift, identified by observing the divergence of reflections within a half-graben structure. This wedge-shaped sequence thickens to the west and pinches out at the Basin Hinge Line eastward. The locations and timings of faults were established and limited by the points where these divergent reflections come to an end.

4.1.2 Transitional Megasequence

The seismic interval SI 2 and SI 3 represent a transitional phase - Barremian and Aptian respectively. In the landward direction, the unconformity is overlapped by parallel and semi-continuous reflections. The break-up unconformity, situated above the reflector package dipping seaward, is covered by a Barremian-early Aptian sedimentary layer across most of the basin (Baby et al., 2018; Kukulus, 2004; Light et al., 1992). This layer indicates the marine inundation of a significant portion of the continental margin and is regarded as part of the transitional phase.

4.1.3 Thermal Sag Megasequence

The seismic interval SI 4 represents Albian (Baby et al., 2018; Kukulus, 2004; Light et al., 1992). The upper part of the structure is marked by a distinct downward-sloping surface identified as a second-order MFS corresponding to the top of Aptian marker (Baby et al., 2018; Kukulus, 2004; Light et al., 1992). The seismic reflections indicate the presence of well-developed clinoforms beneath the shelf. Recent drilled wells

(Murombe and Wingat) in the southern basin have uncovered that these characteristics consist of deposits from carbonate platforms.

The seismic interval SI 5 represents Cenomanian. The stratal arrangement is formed as a result of the development of an aggradational wedge characterized by small-scale clinoforms transitioning upwards to deposits in coastal plains (continuous parallel reflectors). Above Cenomanian (SI 5), there is an erosional unconformity covered by a progradational-aggradational wedge forming high-amplitude clinoforms. Certain reflectors, extending beyond the shelf and overlying the unconformity, are construed as deposits from basin-floor fans.

The seismic interval SI 6, SI 7 and SI 8 represents Turonian, Santonian and Campanian sequences respectively. The primary deposition center of this formation accumulated sediment up to a depth of 1300 meters on the shelf. This is the result of aggradational trends, featuring small-scale clinoforms with low angles that are stacked in the formation.

The seismic interval SI 9 represents base of the Tertiary, Maastrichtian. The base unconformity shows signs of incised valleys in the upstream segment of the margin and erosional truncations in the outer shelf (Baby et al., 2018; Kukulus, 2004; Light et al., 1992). The succeeding layers were deposited toward the basin, as basin-floor fans dominated by sand and substantial slope fans. These are overlain by a wedge that progressed from progradation to aggradation, characterized by higher clinoforms in the central part of the margin as shown in Figure 18. This unconformity signifies a fall in relative sea level below the shelf-break. Canyon incisions took place during the uppermost Cretaceous period in the outer portion of the shelf.

Tertiary

The seismic interval SI 10, SI 11 and SI 12 represents Paleocene, Eocene and Oligocene respectively. An unconformity obscured by a deltaic wedge that progrades and extends over the inner and middle shelf. This wedge is made up of two third-order sequences. The Maximum Regressive Surface (MRS) identified as a wave ravinement surface, evident from the topset truncation of the underlying deltaic wedge (Baby et al., 2018; Kukulus, 2004; Light et al., 1993). The succeeding retrogradational wedge extends over the MRS on the outer shelf and subsequently developed into an aggrading wedge with reflectors that are parallel and continuous (Baby et al., 2018; Kukulus, 2004; Light et al., 1992). The subsequent MSF is observed by a prograding wedge identified as very low-angle clinoforms and a distinct migration of the offlap-break toward the continent (Baby et al., 2018; Kukulus, 2004; Light et al., 1993).

The seismic interval SI 13 represents Miocene. The unconformity is overlain by a progradational wedge showing a sigmoidal convex shape, with the topsets exhibiting an upstream onlap. Despite the sedimentation being primarily characterized by the alternation of calcareous silty claystones and clayey limestones, this unconformity was overlain by a progradational-aggradational wedge where the offlap-break aligns with the shelf-break.

4.2. Seismic facies

In this research domain, a classification of seismic facies was established to enhance the understanding of depositional environments. This categorization includes five groups based on the primary reflection patterns: Parallel, divergent, progradational, irregular, and chaotic.

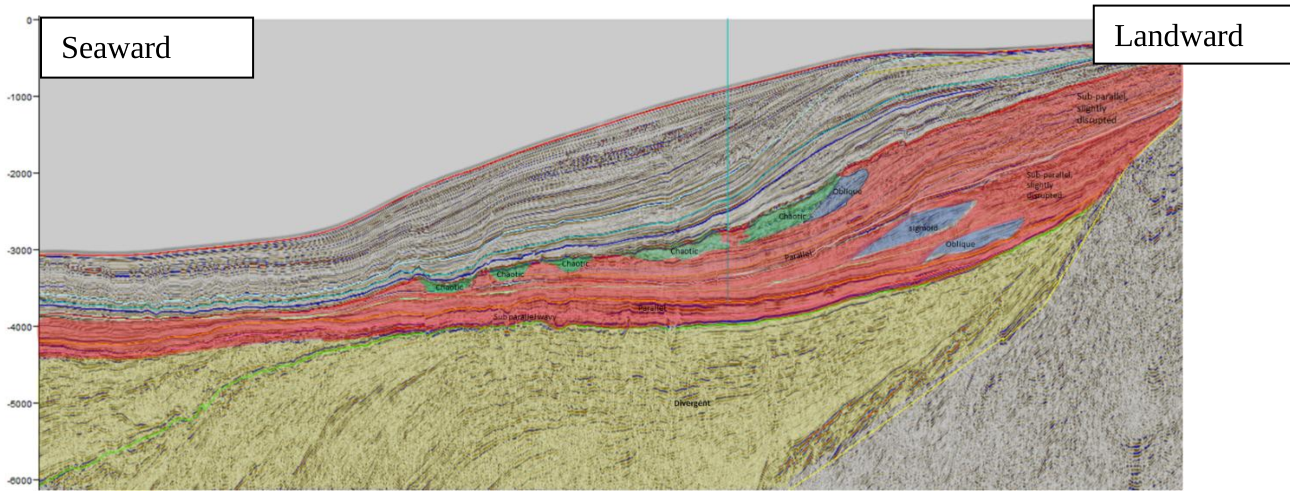

Figure 19: The seismic dip-line ION-GXT NAM -3000_pstm_stk_20150710 displays four distinct seismic facies categories. Interpretations of these facies can vary based on the geological setting. Divergent seismic facies are associated with growth strata within the syn-rift showing seaward dipping reflectors (SDRs) shown in yellow. The section is mostly dominated by sub-parallel–wavy, sub-parallel and slightly divergent, wavy–slightly disrupted, and sub-parallel–slightly disrupted patterns shown in red. Progradational seismic facies of sigmoid and oblique shapes shown in color blue. Chaotic facies discontinuous reflections with low amplitude and lacks consistent geometrical patterns within a unit mostly dominated along the base tertiary (Maastrichtian section) shown in green.

Parallel seismic facies

The seismic facies category characterized by parallel features encompasses reflection geometries that range from continuous to sub-continuous. These include sub-parallel–wavy, sub-parallel and slightly divergent, wavy–slightly disrupted, and sub-parallel–slightly disrupted patterns (see Figure 20). Parallel seismic facies in the Transitional phase and Aptian ranging from subparallel which are slightly disrupted towards the landward (Eastern) to parallel. They are bounded by semitransparent with low amplitude internal reflections.

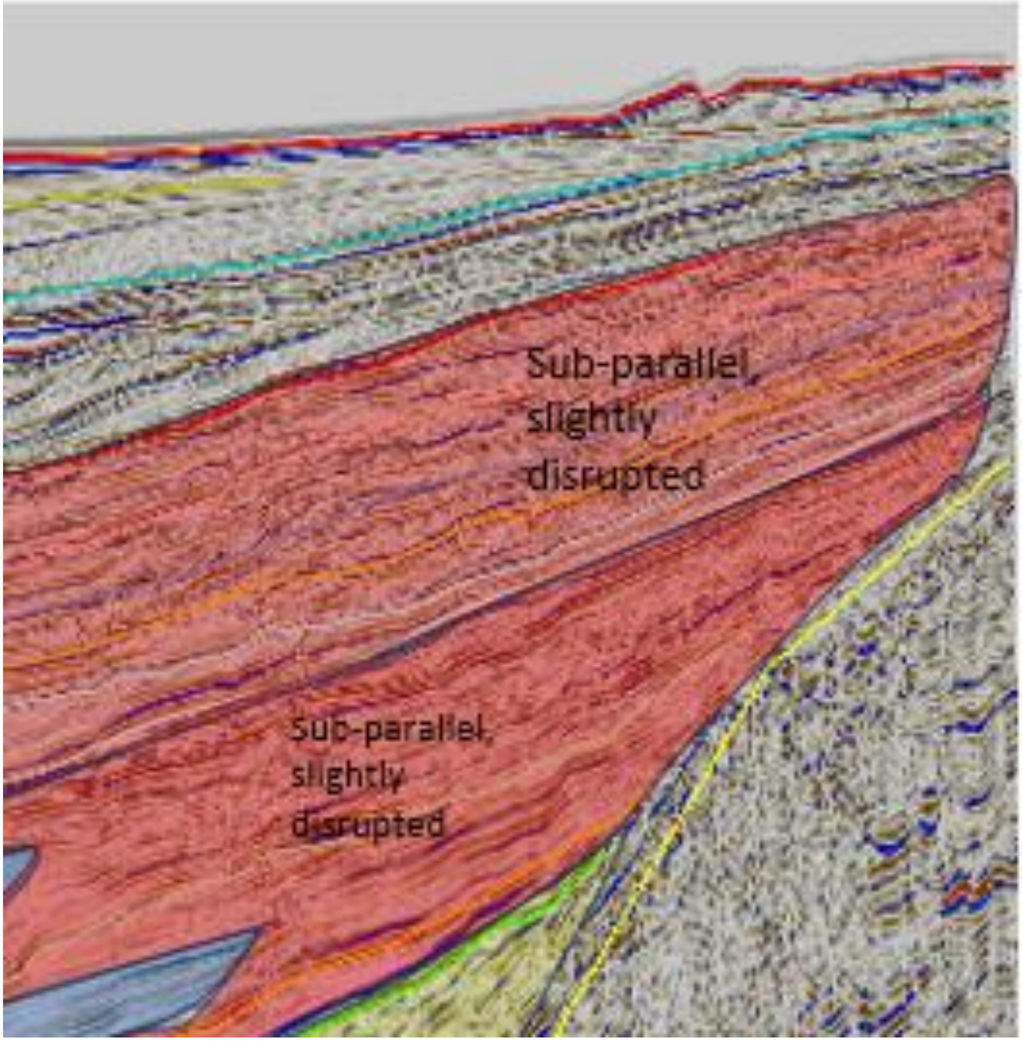

Figure 20: The seismic section exhibits sub-parallel reflectors with are slightly disrupted characterized by continuous reflections of high to moderate amplitude. Situated on the shelf and down basin of the seismic dip line. These facies could signify pelagic to hemipelagic mudstone and turbidite sheets with clay-rich and silt. High amplitude parallel reflector may signify turbidite sheets.

Divergent seismic facies

Divergent seismic facies are visible in the Syn-rift sequence. Faults contributed to the extension of the divergence. It has low to medium amplitude. During the syn-rift phase, there is an anticipation of Continental deposition characterized by the presence of alluvial, fluvial, and potentially lacustrine deposits. These deposits might extend into the transitional sequence as well. This phenomenon elucidates the observation that a substantial portion of the divergent reflections exhibit low continuity or a hummocky pattern. Up to now, no well drilled along the Namibian margin has reached the syn-rift sequence, preventing any calibration from taking place. The characteristic trait signifying its syn-tectonic deposition is evident in the divergent internal structures observed in seismic reflectors, occasionally displaying a fan-like geometry with seaward diverging reflectors exhibiting a high degree of divergence. Within SI 1 (see Figure 21), reflections vary in amplitude from high to medium, displaying a pattern ranging from continuous to discontinuous and demonstrating a divergent nature. These are also displayed by seaward dipping reflectors (SDRs) (see Figure 22). The reflections consistently maintain high continuity, indicating a more uniform or gradually changing deposition process from shallow to deeper marine surroundings.

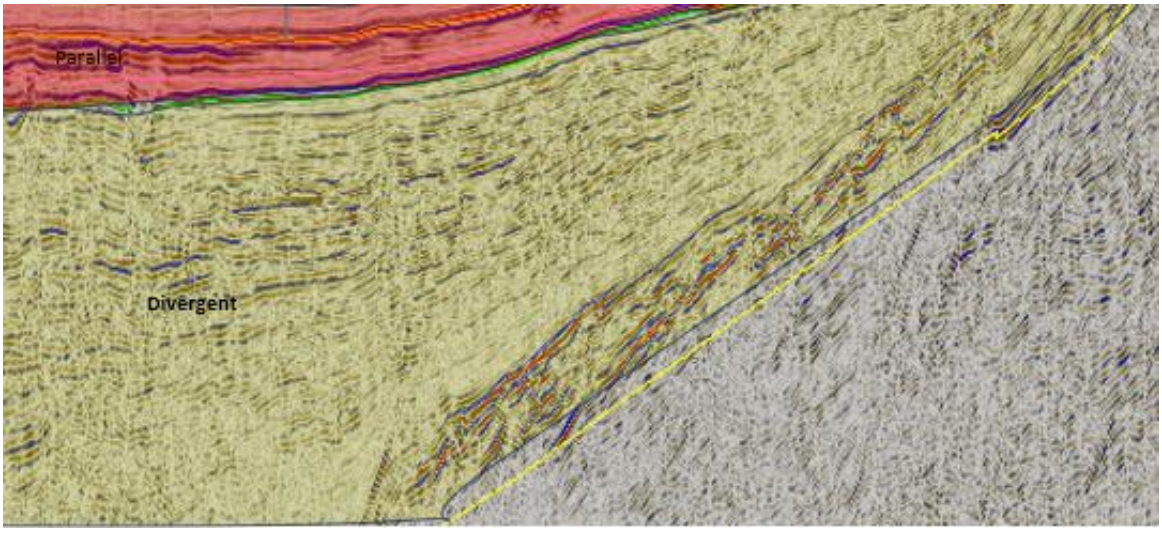

Figure 21: Diverging seismic reflections are observed within the syn-rift sequence. Sedimentation rates increase toward the western main fault. Continental deposition of siliclastics, coupled with extrusive and intrusive volcanism, might account for the varying varying amplitudes and continuity of reflections. This section also shows the seaward dipping reflectors (SDRs).

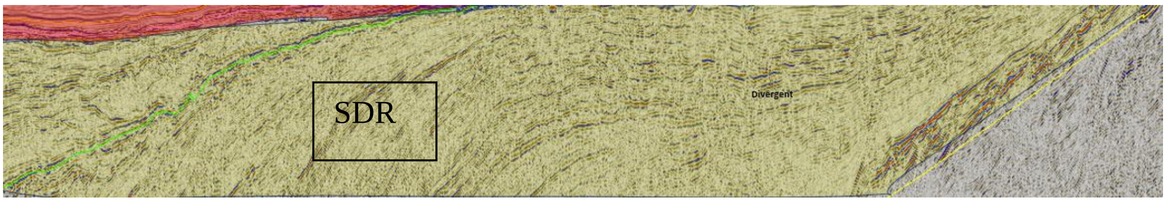

Figure 22: Seaward dipping reflectors (SDRs) within the syn-rift section

Progradational seismic facies

The progradational seismic facies classification encompasses continuous to sub-continuous reflections characterized by high to moderate amplitude. The geometries of these reflections include sigmoid and oblique tangential shapes (see Figure 23). The seismic unit below Albian well top is identified by progradational clinoforms that extend in oblique manner toward the abyssal plain. The facie downlap onto the transitional phase surface, likely representing the outward growth of fluvial fans that terminate in the distant direction. These formations transition towards the west, evolving into more laterally continuous and parallel shallow marine sandstones. The seismic facie westward in the Cenomanian is identified by progradational clinoforms that extend in a sigmoid manner toward the abyssal plain. This facie too extends in a sub parallel which is slightly disrupted seismic reflections.

There is also oblique facie down the Base Tertiary extending into the chaotic facie towards its west and sub parallel slightly disrupted towards the east.

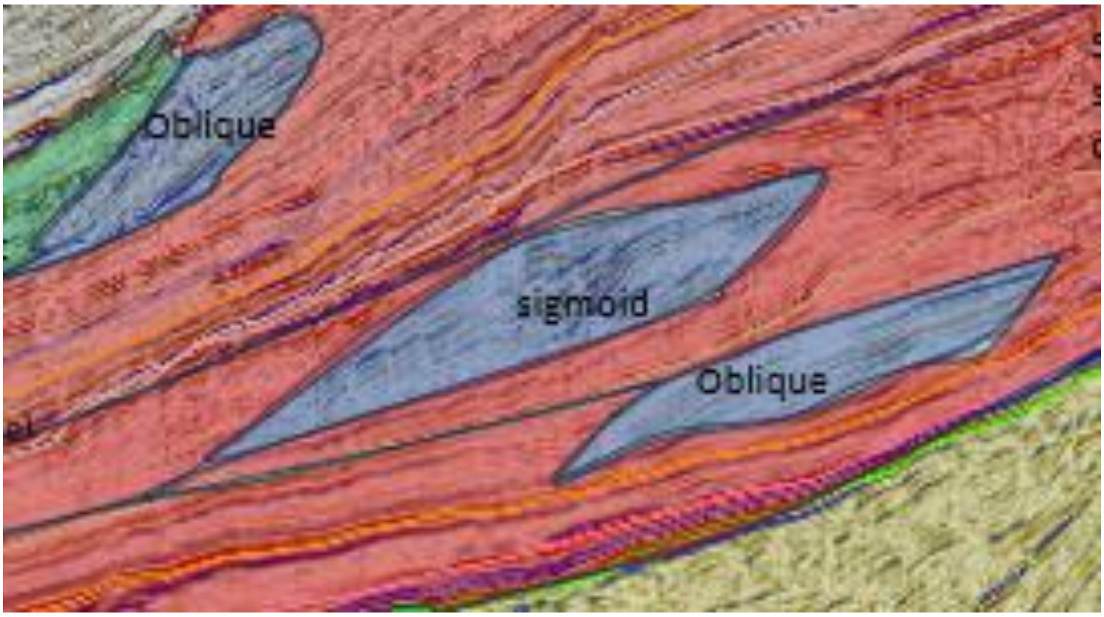

Figure 23: The geometries of progradational facies reflections include sigmoid and oblique tangential shapes. The progradational seismic facies classification encompasses continuous to sub-continuous reflections characterized by high to moderate amplitude. The seismic unit below Albian well top is identified by progradational clinoforms that extend in oblique manner toward the abyssal plain. The seismic facie westward in the Cenomanian is identified by progradational clinoforms that extend in a sigmoid manner toward the abyssal plain.

Chaotic seismic facies

The chaotic seismic facies classification comprises discontinuous reflections with low amplitude and lacks consistent geometrical patterns within a unit (see Figure 24). The seismic facies of that extends from -4000ms to -3500ms shows chaotic facies. Chaotic facies are typically found near distorted and disrupted reflection configurations resulting from post-depositional transport, such as slumping. As a result, the chaotic facies signify the utmost degree of sediment disturbance occurring after deposition.

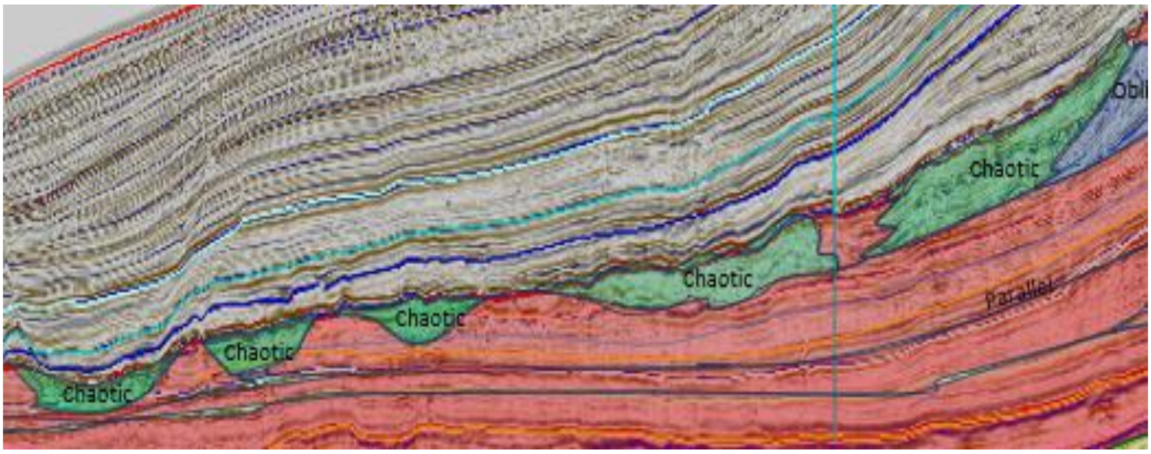

Figure 24: Chaotic facies which comprises of discontinuous reflections with low amplitude and lacks consistent geometrical patterns within a unit mostly dominated along the base tertiary (Maastrichtian section) shown in green. This could result from post-depositional transport, such as slumping.

Thermal History and maturity

Well 2012/13-1 has undergone 1D modeling to comprehend the burial and thermal evolution. This modeling aims to predict the timing of thermal maturation and petroleum generation in the Walvis Basin.

CHAPTER 5: SYNTHESIS AND DISCUSSION

5.1 Sequence recognition and lithofacies prediction

The Cretaceous succession in this study has been sub-divided into 9 Seismic Intervals (SI), delineated based on the identification of 9 seismic stratigraphic surfaces. Ages were attributed from well 2012/13-1 reports. A lithofacies model was developed for seismic line ION-GXT NAM-3000_pstm_stk_20150710, utilizing seismic facies and system tracts, and analogous interpretations of Light et al. (1993), Bagguley and Prosser (1999), Baby et al. (2018), and Joseph (2020).

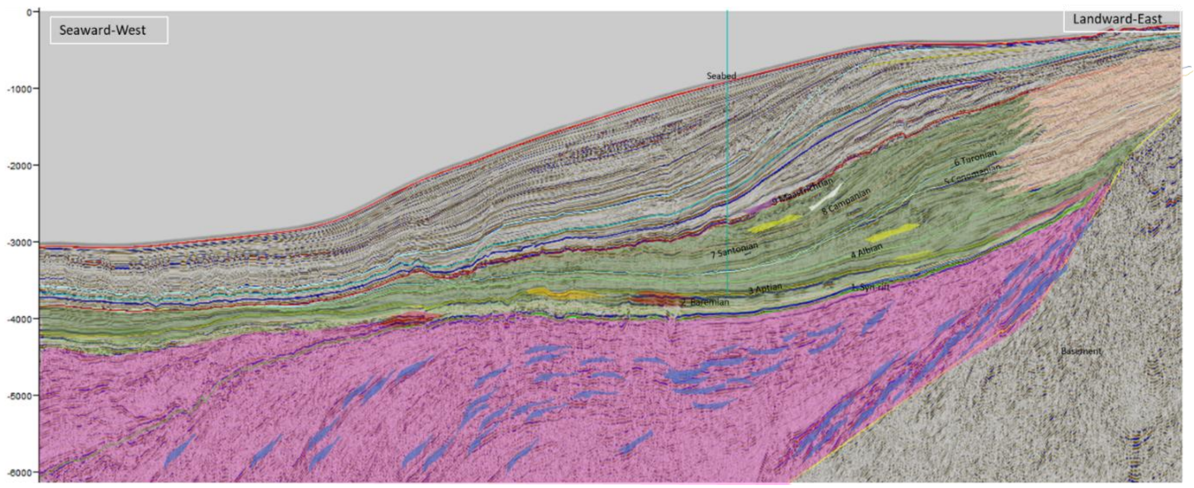

Figure 25: Lithofacies model for seismic dip line ION-GXT NAM-3000_pstm_stk_201507105.

Table 4: Key to the lithofacies model for seismic dip line ION-GXT NAM-3000_pstm_stk_201507105 representing the depositional environment for each color.

Pink	Continental deposits that may include siliciclastics sediments and volcanics with SDRs
Red	Shallow marine carbonates and shale
Black	Shale
Green	Shallow marine sandstones, siltstones, silty claystones and claystones
Yellow	Basin floor fan
White	Slope fan

5.1.1 Syn-rift

Syn-rift unit (SI 1) according to Light et al. (1993), was formed during the Late Jurassic to Hauterivian period. The distinctive feature indicating its syn-tectonic deposition is the presence of divergent internal configurations in seismic reflectors, often displaying an occasional fanning geometry showing seaward divergent reflectors with high degree of divergence. Reflections in SI 1 vary in amplitude from high to medium, exhibiting a pattern that ranges from continuous to discontinuous and shows a divergent nature. The Syn-rift interval (SI 1) is mainly comprised of continental deposits that may include siliciclastics sediments such as sandstones, conglomerates, overbank fines, lacustrine shales, siltstones etc. Moreover, the Namibian Margin is viewed as a volcanic passive margin (Gladczenko et al., 1998) and therefore, volcanics deposits of late Jurassic to early Cretaceous age, such as lavas, sills, dykes etc are also expected to be extensively spread across the syn-rift interval (SI 1). The intersection of the syn-rift unit at the Kudu field proved the presence of siliciclastics and volcanics in the Syn-rift, as a reservoir interval made up of nearshore and aeolian sandstones intercalated with basalts was intersected.

5.1.2 Transitional Phase

SI 2 was deposited during Hauterivian to Barremian age and possess an average thickness of 125 milliseconds at the well 2012/13-1 site. SI 2 represents a breakup unconformity that serves as a distinctive marker representing a shift from the rift phase to the drift (thermal sag) phase. The break-up unconformity is well represented by a regional onlap of SI 2 onto SI 1. The interval is characterized by high to medium amplitude reflections that are continuous to discontinuous. Furthermore, the interval is characterized by a divergence nature, indicative of growth strata. During this interval a transition from lacustrine to restricted marine conditions is recognized. Marine conditions started to establish during the first flooding of the South Atlantic. Restricted circulation in the slowly widening South Atlantic facilitated anoxic bottom waters and deposition of organic matter rich shales. The continuous reflections are understood to represent shallow marine sandstones, siltstones and claystones. Carbonates resting on mafic volcanics have been intersected in the Murombe-1 well in the southern Walvis Basin. Therefore, the high amplitude events interpreted in SI 2 likely represents the latter intersected carbonates and volcanics. Carbonates occurring where Aptian shales drape over structural highs could provide high quality reservoirs of excellent porosity. Continuous reflection patterns are interpreted on the lower slope of the SI 2, suggesting a uniform deposition of deeper marine shales. This aligns with observations made in wells located in the Orange (Kudu wells) and Murombe well, where kerogenous shales were intersected.

SI 3 was deposited during the Aptian age. The overall down dip curvature of the reflections in the Aptian Interval (SI 3) indicates development of a shelf-slope bathymetry with slightly increased sedimentation rate towards the deeper basin. The interval is overall aggradational with a subtle downlap surface occurring in the upper section of this interval. SI 3 is landward and onlapping onto the basement indicating a transgressive development of the interval and likely implying that restricted coarser siliciclastics were deposited onto shelf, with few mass flows (turbidites/debrites) reaching the deeper basin. High Amplitude events are also interpreted as shallow marine carbonates and volcanics and carbonates occurring where Aptian shales drape over structural highs could provide high quality reservoirs of excellent porosity. Charge excess is very likely considering their proximity/juxtaposition to the Aptian shales, and therefore those carbonate highs may be primary leads. The continuous medium to high amplitude events outside structural highs are interpreted as a possible mixture of finer sediments (shales) with carbonates; those carbonates are likely of lower reservoir quality than those deposited on the highs.

5.1.3 Thermal Sag

The seismic reflectors observed on the shelf display a predominantly parallel orientation, although there are indications of coastal onlap in some areas. Towards the east, they appear somewhat more or less discontinuous or semi-continuous, featuring intervals of relative tranquility interbedded with layers of high-energy shoreline to shallow marine sands, along with inter-laminated shales, and perhaps thin limestones. In the western part of the shelf, there are predominantly continuous reflectors, interspersed with calmer and translucent interbeds. These indicate the presence of lower-energy sands and shales situated on the outer shelf, extending beyond the influence of wave energy and inshore currents as studied by (Light et al., 1993).

SI 4 was deposited during the Albian time, approximately 125 million years ago. SI 4 correlates to a hiatus interpreted in Baby et al (2018) that is associated with major environmental transition from deeply anoxic sediments below to well-oxygenated mudstones above, spanning from upper Aptian to the Late Albian. Furthermore, SI 4 marks the initiation of basin distinction of the margin into a shelf, slope and deeper basin. The interval was deposited mostly in a shallow marine setting with limited accommodation space as the full passive margin geometry did not yet reach maturity.

At Well 2012/13-1 bathymetry, SI 4 holds an average thickness of 212 milliseconds. The characteristics of the interval include reflections of medium to low amplitude that are predominantly continuous. This aligns with a slightly oblique configuration of reflections mapped on the shelf (Figure 25 and Table 4). Events with high amplitude oblique reflections are likely associated with carbonate activities that are also mentioned in Baby et al (2018). This interval is mostly dominated by claystone and silty claystone especially at the area intersected by the 2012/13-1 well.

SI 5 was deposited during Cenomanian periods, approximately 100–93.5 million years ago with thickness of 96 milliseconds at the 2012/13-1 well area. The characteristics of SI 5 includes sub-parallel and slightly disrupted reflections of medium to low amplitude that are predominantly continuous. Sigmoidal internal configurations with medium to low amplitude reflections are also mapped below the shelf to the upper slope. Furthermore, SI 5 is interpreted as a Low System Tract (LST) and Progradational with downlap against the Albian surface at some areas.

The stratal arrangement of the SI 5 consists of aggradational wedge of sediment accumulation characterized by small-scale clinoforms transitioning into deposits found along coastal plains, which appear as continuous parallel reflections. On the mid and lower slope lowstand fan (basin floor fan) and lowstand wedge geometries are recognized in SI 5 (Table 4 and Figure 25) a slightly mounded feature displaying an aggradational stacking pattern immediately at the base-of-slope is a lowstand fan. Downlapping on the lowstand fan are the Lowstand wedges consisting of progradational parasequences onlapping successively onto the slope. The Lowstand Wedge has been likely formed in response to the rise of sea level also indicated by the mfs on top of the Cenomanian interval. The more parallel reflections are interpreted as more or less continuous turbidite sheets that are interbedded with deep marine hemipelagic mudrocks and shales.

The noticeable continuous and intricate sigmoidal pattern on the upper to lower slope of SI 5, suggests that this area represents a high-energy shallow marine setting conducive to the deposition of sand. The continuous reflections are understood to represent open marine and outer neritic formations, specifically sandstones, silty claystones and siltstones with the outer shelf lithology dominated by silty claystones. Cenomanian/ Turonian marine carbonaceous claystones have good source rock potential present in the central and northern Walvis Basin.

SI 6 and SI 7 were deposited during Turonian and Santonian age. These intervals are characterized by subparallel to transparent reflections with moderate amplitudes on the shelf. Furthermore, SI 6 and SI 7 are characterized by several discontinuities that are representing a stacked succession of progradational buildouts with superseding periods of transgression that developed during the Late Cretaceous (Light et al., 1993). This sub-parallel to transparent seismic character could relate to sediment instability and dewatering, possibly due to high sedimentation rates and a high proportion of fine-grained (silt, clay-rich) sediment. These reflections may also be interpreted as pelagic mudstones and turbidite sheets, displaying a slightly disrupted pattern.

SI 8 and SI 9 were laid down during Campanian and Maastrichtian period respectively. The intervals are characterized by Clinoform bottomsets that are corresponding to SI 9 Downlapping downslope on SI 8, creating subparallel reflections with moderate amplitudes. These reflections are interpreted as pelagic mudstones and turbidite sheets, displaying a slightly disrupted pattern as in SI 6 to SI 8. The deposition during the highstand phase is deduced from shelf progradation, as indicated by the downlap surface creating a slope fan. It also created a whole separate system tract consisting of lowstand and transgressive system tract.

The location of the shelf in SI 8 and SI 9 is well defined by the clinoform geometries with preserved top-sets, and prograding distal down-lap on the Santonian unconformity also interpreted in Baby et al (2018). This basinward shift of the shelf break and preservation of the top-sets points to moderately high sediment supply during the early sea-level rise of the LST. Reflections up-section are more aggrading, therefore, defining a transgressive surface. Pronounced prograding clinoforms are lacking downslope and this could be possibly due to low sediment supply. Sandstones are anticipated to be within the clinoforms, with the downdip turbidites expected to be less sand-prone compared to the preceding lowstand turbidites.

The outer section of the Walvis Basin is characterized by continuous, parallel reflections intercalated with transparent zones, indicating the deposition of low-energy, deep marine shale (Light et al., 1993). The Maastrichtian unconformity records a notable decline in relative sea level below the shelf-break. Canyon incisions took place in the outer section of the shelf, likely initiated by shelf instability during the late Cretaceous period.

5.2 Petroleum system elements

To interpret the petroleum system elements for the Cretaceous period, a petroleum system model based on the lithofacies model showing the distribution of source rock, reservoir rock, seal rock and trap lithologies has been created for seismic dip line ION-GXT NAM-3000_pstm_stk_20150710 (Figure 26).

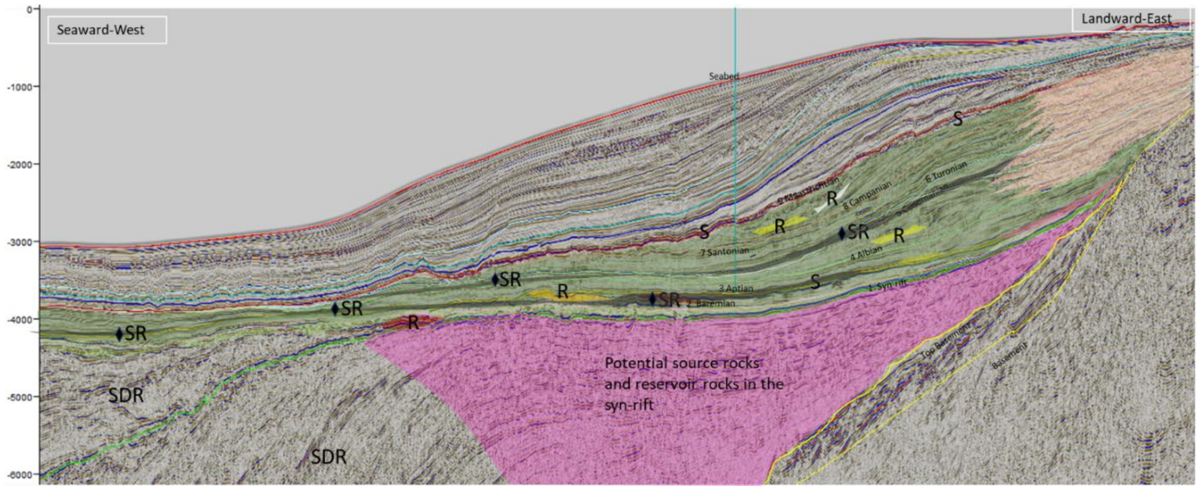

Figure 26: Theoretical illustration of the distribution of source rocks represented as SR, reservoir rocks represented as R, trap represented as T and seal rocks represented as S may have developed in the cretaceous section of Walvis Basin.

5.2.1 Source Rocks

Barremian to Albian period source rocks

As depicted in the study, the deposition of potential source rocks took place in the Lower Cretaceous period, spanning from the Barremian to the Turonian times. Prominent are three distinct parallel high-amplitude horizons believed to be the Aptian/Albian source rocks although not intersected by well 2012/13-1. The Walvis Basin, as indicated by wells 1911/10-1, 1911/15-1, 2012/13-1, and 2213/6-1, has not encountered Barremian/Aptian source rocks. However, given their presence in Angolan waters and the Cape Basin, Kukulus (2004) and Bray et al. (1998) anticipate a broad distribution of these source rocks along the Namibian margin. The Wingat-1 and Murombe-1 wells in the Southern Walvis Basin has successfully encountered the Aptian/Albian source rock well known as the Kudu Shale. In this study, there are semi-continuous and continuous reflections present in transitional seismic units SI 2 and SI 3, which align with shale layers that extend laterally. SI 3 representing the Aptian age, shows a general highstand system track (HST) pattern with retrogradation and hosts a well-preserved MFS (maximum flooding surface) top, making it a promising prospect for containing organic-rich shales that could serve as valuable source rocks.

Cenomanian to Turonian source rock period

Cenomanian/Turonian. Cenomanian/Turonian marine carbonaceous claystones exhibiting significant source rock potential which has been proven to exist in the central and northern Walvis Basin from wells 2012/13-1, 1911/15-1, and 1911/10-1. The continuous reflections in SI 5 and SI 6 could signify pelagic to hemipelagic mudstone and turbidite sheets with clay-rich and silt are interpreted as formations from open marine and outer neritic formations, comprising mainly sandstones, silty claystones, and siltstones. Specifically, in the central Walvis Basin, well 2012/13-1 offers direct access to dark, organic-rich claystones. The outer shelf lithology is dominated by silty claystones with partial carbonaceous content from the Late Cenomanian/Turonian period, drilled at depths ranging between 3411 m and 3663 m.

The Cenomanian-Turonian interval encompasses the primary sections identified as source rocks within the well 2012/13-1. In general, total organic carbon (TOC) levels span from 0.63% to 5.86%, averaging at 2.02% (Well 2012/13-1 Sasol Geochemistry report). The upper portion of this interval, corresponding to the earliest Turonian period, exhibits the highest TOC values. The greatest levels of organic carbon (TOC) reaching 5.45% were detected within the depth range of 3555m to 3567m, corresponding to the earliest Turonian period. This section comprises dark grey mudstone with varying degrees of carbon content, abundant moderately pyritic sapropelic amorphous organic matters. Cenomanian/ Turonian marine carbonaceous claystones have good source rock potential present in the central and northern Walvis Basin.

Widespread occurrences of marine anoxic black shales from the Cenomanian to Turonian period are observed in the South Atlantic. The black organic-rich shale from the Cenomanian/Turonian period is recognized as a source rock of global significance linked to the occurrence of the Ocean Anoxia Event (Forster et al., 2008). This event led to the accumulation and preservation of extensive mudstone deposits characterized by high total organic carbon (TOC) content across the globe.

5.2.2 Reservoir Rocks

Reservoir rocks, such as Carbonates from the Barremian to Aptian period and turbidite sandstones from the Upper Cretaceous, are considered as potential reservoir rocks in the Walvis Basin. The Walvis Basin is home to extensive exploration opportunities, featuring high-quality reservoirs located at the Cenomanian and Santonian levels, namely, the turbidite sands channel known as Baobab sands of Santonian age. The Santonian turbidite sand channels is a 242-meter section with 15% net-to-gross ratio and an average porosity of 19%. The Santonian turbidite sands exhibit brighter amplitude section is represented by SI 7 in Figure 26.

Despite being water wet, the Late Cretaceous turbidites have reservoir sands of high quality showing sub-parallel to transparent seismic character observed in SI 6 to SI 9

(Figure 26) could be linked to sediment instability and dewatering, as a result of high sedimentation rates and a high proportion of fine-grained (silt, clay-rich) sediments(Light et al., 1993). The seismic reflections may also be interpreted as pelagic mudstones and turbidite sheets, because of a slightly disrupted pattern.

Well 2012/13-1 has encountered significant sandstone sections from 2598 meters to 2969 meters, Upper Campanian/Maastrichtian in age (SI 8 to SI 9) (Figure 26). This interval is believed to have reservoir rock of potentially high quality values of up to 21% porosity with a negligible clay content (Kukulus, 2004). Therefore, the reservoir quality may be interpreted as a good reservoir. Maastrichtian deep marine fan sands and base Tertiary reef-like features may be possible reservoirs that have been fed through the gas chimneys.

5.2.3 Seal Rocks

A sufficient seal might be a crucial element that completes the petroleum system. In certain shelfal wells, substantial clastic sequences have been identified, containing minimal shale to serve as a sealing layer for the sandstone reservoirs (Baby et al., 2018). However. a risk of no seal on the Maastrichtian section may exist since it is overlain by slope fans.

Potential seals within the syn-rift sequence (SI 1) includes lacustrine shales, thin evaporites, and impermeable igneous formations such as lava flows and volcanics. In the Barremian-Aptian period (SI 2- SI 3), marine shales, some of which may act as source rocks, and effective seals.

5.2.4 Trap Rocks

The extensive volcanic activity associated with the Tristan mantle plume and the deposition of syn-rift sediments largely conceal any rift-related structures within the

Walvis Basin. Nevertheless, the presence of sand layers interbedded between individual lava flow sheets might create opportunities for stratigraphic pinch-out traps, albeit potentially affected by the breakup unconformity.

The onlapping of the early drift sediments (SI 2 & SI 3) onto the hinge zone presents significant opportunities for the formation of stratigraphic traps (Figure 26). Hydrocarbons originating from the Barremian/Aptian period were discovered in the Kudu wells and offshore Angola (Baby et al., 2018; Kukulus, 2004; Sibeya, 2014). Hydrocarbons generated in the early drift section and older could potentially be trapped in areas where stratigraphic pinch-out or onlapping occurs in updip locations as seen in Figure 26.

Reservoirs found during the latter stages of post-rift evolution may contain hydrocarbons originating from both the organic-rich shales in the Barremian/Aptian and Cenomanian/Turonian periods. The Maastrichtian deep marine fan sands exhibit good reservoir qualities and might exhibit pinch-out patterns (Figure 25 and Figure 26). Additionally, the mounded reef-like structures associated with the base tertiary unconformity, as mentioned earlier, could serve as excellent potential traps due to their anticlinal nature.

Multiple channel systems from the Cenomanian period, distinguished by both structural and stratigraphic trap types, have been identified and mapped within the Lower Cretaceous basin floor/slope fan systems in the Walvis Basin.

This study focused on examining 2D section of the central area of the Walvis Basin. The goal is to carry out a comprehensive assessment of the hydrocarbon potential by incorporating all relevant data obtained from both wells and seismic studies to identify and delineate the key seismic sequences of the basin to establish the various seismic facies and predict the major petroleum system elements within the basin (source, reservoir, traps etc).

CHAPTER 6: CONCLUSIONS AND RECOMMENDATIONS

The 2D seismic interpretation of the central Walvis Basin has enabled the identification and delineation of nine distinct seismic stratigraphic intervals within the Cretaceous succession, highlighting the complex stratigraphic and depositional history of the basin. Integration of seismic facies analysis, systems tract interpretation, and analog comparisons with adjacent basins (Lüderitz Basin and Orange Basin) has provided valuable insights into the basin's lithofacies distribution and petroleum system development.

The study confirms the presence of multiple potential source rock intervals, particularly the Aptian/Albian and Cenomanian-Turonian formations. While the Aptian source is geochemically validated as a marine oil-prone unit encountered in several wells, the Cenomanian-Turonian source, though laterally extensive and exhibiting favorable TOC values, presents uncertainties regarding its thermal maturity. This duality in source rock characterization suggests variability in hydrocarbon generation potential across the basin.

Reservoir prediction within the pre-breakup section remains a critical aspect of exploration, especially in light of the basin's volcanic overprint. The presence of potential Lower Aptian to Lower Albian carbonate and siliciclastic units within structurally favorable settings offers prospective targets, albeit with a necessity for refined stratigraphic and petrophysical evaluation.

The unsuccessful well outcomes can be attributed to the absence of certain elements or processes in the petroleum system, with the lack of reservoir or charge being the more prevalent causes of failure. The primary risks identified, namely, reservoir presence and effective hydrocarbon charge, highlight the need for 3D seismic studies and targeted drilling informed by integrated basin modeling. The findings of this study reaffirm the Walvis Basin's potential as a frontier petroleum province and underscore the importance of continued exploration supported by a systems-based geological approach.

To further advance the understanding of the Walvis Basin's hydrocarbon potential, this study recommends a focused integration of available 3D seismic data, particularly over study area, into ongoing stratigraphic and structural analysis. While this study relied on 2D seismic data to identify nine seismic stratigraphic intervals and interpret depositional facies and petroleum system elements, 3D seismic offers significantly improved vertical and lateral resolution. Moreover, the development of an integrated 3D petroleum systems model is strongly recommended. This model should incorporate all available well, seismic, and geochemical data, including TOC content and thermal maturity values, to simulate hydrocarbon generation, migration pathways, and accumulation zones. The inclusion of 3D seismic data in such a model would drastically improve structural realism and stratigraphic accuracy, resulting in a more predictive understanding of play risks across the basin.

REFERENCES

Al-Masgari, A. A.-S., Elsaadany, M., Latiff, A. A., & Imran, Q. S. (2021). A guideline for seismic sequence stratigraphy interpretation. *J Eng Appl Sci*, *16*, 165–183.

Al-Masgari, A. A.-S., Elsaadany, M., Rahman, A., Hermana, M., Latiff, A. H. A., Babikir, I., Adeleke, T. O., Imran, Q. S., & Appiah, N. (2006). *A guideline for seismic sequence stratigraphy interpretation*.

Baby, G., Guillocheau, F., Morin, J., Ressouche, J., Robin, C., Broucke, O., & Dall'Asta, M. (2018). Post-rift stratigraphic evolution of the Atlantic margin of Namibia and South Africa: Implications for the vertical movements of the margin and the uplift history of the South African Plateau. *Marine and Petroleum Geology*, *97*, 169–191.

Bagguley, J., & Prosser, S. (1999). The interpretation of passive margin depositional processes using seismic stratigraphy: Examples from offshore Namibia. *Geological Society, London, Special Publications*, *153*(1), 321–344.

Blaich, O. A., Faleide, J. I., & Tsikalas, F. (2011). Crustal breakup and continent-ocean transition at South Atlantic conjugate margins. *Journal of Geophysical Research: Solid Earth*, *116*(B1).

Blaich, O. A., Faleide, J. I., Tsikalas, F., Gordon, A. C., & Mohriak, W. (2013). Crustal-scale architecture and segmentation of the South Atlantic volcanic margin. *Geological Society, London, Special Publications*, *369*(1), 167–183. https://doi.org/10.1144/SP369.22

Bray, R., Lawrence, S., & Swart, R. (1998). Source rock, maturity data indicate potential off Namibia. *Oil and Gas Journal*, *96*(32). https://www.osti.gov/biblio/634725

Brazil Petro Studies. (2022, February 16). *Namibia oil and gas potential – a sleeping giant is waking up*. Retrieved July 19, 2025, from https://brazilpetrostudies.com.br/2022/02/16/namibia-oil-and-gas-potential-a-sleeping-giant-is-waking-up/

Chauvet, F., Sapin, F., Geoffroy, L., Ringenbach, J.-C., & Ferry, J.-N. (2021). Conjugate volcanic passive margins in the austral segment of the South Atlantic–Architecture and development. *Earth-Science Reviews*, *212*, 103461.

Clemson, J., Cartwright, J., & Booth, J. (1997). Structural segmentation and the influence of basement structure on the Namibian passive margin. *Journal of the Geological Society*, *154*(3), 477–482.

Dingle, R. V. (1992). Structural and sedimentary development of the continental margin off southwestern Africa. *Communications of the Geological Survey of Namibia*, *8*, 35–43.

Dingle, R. V., Siesser, W. G., & Newton, A. R. (1983). *Mesozoic and Tertiary geology of southern Africa*. AA Balkema Rotterdam.

Eco Atlantic Oil & Gas. (n.d.). *Namibia – Eco (Atlantic) Oil & Gas Plc* [Web page]. Retrieved July 19, 2025, from https://www.ecooilandgas.com/projects/namibia/

Fernandes, F. M., Chemale Jr, F., Lelarge, M. L. M., & Jr, J. L. L. (2003). *Thermo-tectonic evolution of the Purros Shear Zone and its implications in Walvis Basin, NW Namibia*.

Forster, A., Kuypers, M. M., Turgeon, S. C., Brumsack, H.-J., Petrizzo, M. R., & Damsté, J. S. S. (2008). The Cenomanian/Turonian oceanic anoxic event in the South Atlantic: New insights from a geochemical study of DSDP Site 530A. *Palaeogeography, Palaeoclimatology, Palaeoecology*, *267*(3–4), 256–283.

Futalan, K., Mitchell, A., Amos, K., & Backe, G. (2012). Seismic facies analysis and structural interpretation of the Sandakan sub-basin, Sulu Sea, Philippines. *AAPG Search and Discovery Article*, *30254*.

Gladczenko, T. P., Skogseid, J., & Eldhom, O. (1998). Namibia volcanic margin. *Marine Geophysical Researches*, *20*, 313–341.

Hall, S. A., Bird, D. E., McLean, D. J., Towle, P. J., Grant, J. V., & Danque, H. A. (2018). New constraints on the age of the opening of the South Atlantic basin. *Marine and Petroleum Geology*, *95*, 50–66.

Hartwig, A. (2014). *Hydrocarbon migration and leakage dynamics of the Orange Basin, South Africa*. https://depositonce.tu-berlin.de/bitstream/11303/4459/1/hartwig_alexander.pdf

Joseph, R. (2020). *Seismic stratigraphy and burial history for source and reservour prediction in the Luderitz basin, license blocks 2412B and 2413B, offshore Namibia* [PhD Thesis]. University of Namibia.

Kabaca, E. (2018). *Seismic stratigraphic analysis using multiple attributes-an application to the f3 block, offshore Netherlands* [PhD Thesis, University of Alabama Libraries]. https://ir.ua.edu/bitstream/handle/123456789/3693/file_1.pdf?sequence=1

Koopmann, H., Franke, D., Schreckenberger, B., Schulz, H., Hartwig, A., Stollhofen, H., & di Primio, R. (2014). Segmentation and volcano-tectonic characteristics along the SW African continental margin, South Atlantic, as derived from multichannel seismic and potential field data. *Marine and Petroleum Geology*, *50*, 22–39.

Kuhlmann, G., Adams, S., Anka, Z., Campher, C., Di Primio, R., & Horsfield, B. (2011). 3D petroleum systems modelling within a passive margin setting, Orange Basin, blocks 3/4, offshore South Africa–implications for gas generation, migration and leakage. *South African Journal of Geology*, *114*(3–4), 387–414.

Kukulus, M. (2004). *A quantitative approach to the evolution of the central Walvis Basin offshore NW-Namibia: Structure, mass balancing, and hydrocarbon potential* [PhD Thesis]. Universität Würzburg.

Le, A. N. (2012). *Stratigraphic evolution and plumbing system in the Cameroon margin, West Africa*. The University of Manchester (United Kingdom).

Light, M. P. R., Maslanyj, M. P., & Banks, N. L. (1992). New geophysical evidence for extensional tectonics on the divergent margin offshore Namibia. *Geological Society, London, Special Publications*, *68*(1), 257–270.

Light, M. P. R., Maslanyj, M. P., Greenwood, R. J., & Banks, N. L. (1993). Seismic sequence stratigraphy and tectonics offshore Namibia. *Geological Society, London, Special Publications*, *71*(1), 163–191.

Miller, R. M. (2008). *The geology of Namibia* (Vol. 1). Ministry of Mines and Energy, Geological Survey.

Mitchum Jr, R. M., Vail, P. R., & Thompson III, S. (1977). *Seismic stratigraphy and global changes of sea level: Part 2. The depositional sequence as a basic unit for stratigraphic analysis: Section 2. Application of seismic reflection configuration to stratigraphic interpretation*.

Mohammed, M., Paton, D., Collier, R. E. L., Hodgson, N., & Negonga, M. (2017). Interaction of crustal heterogeneity and lithospheric processes in determining passive margin architecture on the southern Namibian margin. *Geological Society, London, Special Publications*, *438*(1), 177–193.

National Petroleum Corporation of Namibia. (2016). *Exploration & production booklet*. Windhoek, Namibia: NAMCOR.

Parvin, A., & Woobaidullah, A. S. M. (2019). Incorporation of Sequence Stratigraphy in Gas Reservoir Correlation: A Case Study. *Journal of the Asiatic Society of Bangladesh, Science*, *45*(2), 209–216.

Ryberg, T., Haberland, C., Haberlau, T., Weber, M. H., Bauer, K., Behrmann, J. H., & Jokat, W. (2015). Crustal structure of northwest Namibia: Evidence for plume-rift-continent interaction. *Geology*, *43*(8), 739–742.

Sasol Petroleum (Namibia) Pty Ltd. (1997). *A high-resolution biostratigraphic study of Sasol Well 2012/13-1, Walvis Basin, offshore Namibia* [Internal report]. Sasol Strong Room Inventory.

Serratt, H., Domingues Teixeira, C., Girelli, T. J., De Souza, M. K., Rodrigues Vargas, M., Moreira Silva, A., & Chemale, F. (2022). Seaward-Dipping Reflector Influence on Seafloor Magnetostratigraphy—A Pelotas Basin View. *Geophysical Research Letters*, *49*(23), e2022GL100382. https://doi.org/10.1029/2022GL100382

Sibeya, V. (2014). *Seismic study of the Orange Basin, offshore Namibia and its relecance for Hydrocarbon system analysis* [PhD Thesis, University of Namibia]. https://repository.unam.edu.na/handle/11070/1989

Taner, M. T., Koehler, F., & Sheriff, R. E. (1979). Complex seismic trace analysis. *Geophysics*, *44*(6), 1041–1063.

Tower Resources PLC. (2020, July 28). *Tower updates Namibia work program and resources*. Retrieved July 19, 2025, from [Tower Resources website]

Vail, P. R. (1987). *Seismic stratigraphy interpretation using sequence stratigraphy: Part 1: Seismic stratigraphy interpretation procedure*.

Vail, P. R., Mitchell Jr, R. M., Sangree, J. D., & Thompson III, S. (1975). *Eustatic cycles from seismic data for global stratigraphic analysis*.

Van Wagoner, J. C., Mitchum, R. M., Campion, K. M., & Rahmanian, V. D. (1990). *Siliciclastic sequence stratigraphy in well logs, cores, and outcrops: Concepts for high-resolution correlation of time and facies*.

Wen, Z., Jiang, S., Song, C., Wang, Z., & He, Z. (2019). Basin evolution, configuration styles, and hydrocarbon accumulation of the South Atlantic conjugate margins. *Energy Exploration & Exploitation*, *37*(3), 992–1008.

Wu, H., Khan, M., & Song, P. (2019). Sequence Stratigraphy towards its standardization—An important scientific scheme. *E3S Web of Conferences, 131*, 01034. https://ui.adsabs.harvard.edu/abs/2019E3SWC.13101034W/abstract

Yugyè, J. A., Chavom, B. M., Chima, K. I., N'nanga, A., Biouélé, S. E. A., Nkoa, P. E. N., & Ngos III, S. (2022). Seismic-stratigraphic analysis and depositional architecture of the Cenozoic Kribi-Campo sub-basin offshore deposits (Cameroon): Seismic attributes approach and implication for the hydrocarbon prospectivity. *Journal of African Earth Sciences*, *194*, 104621.

APPENDICES

Appendix 1: Ethical Clearance

UNAM
UNIVERSITY OF NAMIBIA

ETHICAL CLEARANCE CERTIFICATE

Ethical Clearance Reference Number: SOC/0008 **Date: 29 September 2022**

This Ethical Clearance Certificate is issued by the University of Namibia Ethics Committee (REC) in accordance with the University of Namibia's Research Ethics Policy and Guidelines. Ethical approval is given in respect of undertakings contained in the Research Project outlined below. This Certificate is issued on the recommendations of the ethical evaluation done by the ethics committee.

Title of Project: SEISMIC STRATIGRAPHIC ANALYSIS FOR THE CHARACTERISATION OF PETROLEUM SYSTEM ELEMENTS, WALVIS BASIN, OFFSHORE NAMIBIA

Principal researchers: Ester David

Staff Number/ Student number: 201136562

Remarks: None

Centre for Research Services

Take note of the following:

1. Any significant changes in the conditions or undertakings outlined in the approved Proposal must be communicated to the ethics committee. An application to make amendments may be necessary.
2. Any breaches of ethical undertakings or practices that have an impact on ethical conduct of the research must be reported to the ethics committee
3. The Principal Researcher must report issues of ethical compliance to the ethics committee (through the Chairperson) at the end of the Project or as may be requested by the ethics committee
4. The ethics committee retains the right to:

i) Withdraw or amend this Ethical Clearance if any unethical practices (as outlined in the Research Ethics Policy) have been detected or suspected,

ii) Request for an ethical compliance report at any point during the course of the research.

The ethics committee wishes you the best in your research.

Dr Josefina T Hamutoko (Chairperson Decentralized Ethics Committee)

Prof. Davis Mumbengegwi (Head, Multidisciplinary Research)

Appendix 2: Table of stratigraphic interval description for SI 1 to SI 9 (Baby et al., 2018; Kukulus, 2004; Light et al., 1993)**.**

Unit/ Surface	**Main characteristic**	**Seismic facies Shelf**	**Seismic facies Slope**	**Seismic facies Basin floor**	**Tentative correlation with well 2012/13-1 (ages, SBs, MFS)**	**Lithology in well 2012/13-1**	**Interpretation of unit/surface**	**Lithology prediction Shelf**	**Lithology prediction Slope**	**Lithology prediction Basin floor**
1	Syn-rift, divergence pattern	Divergent	divergent	Divergent	Absent	Absent				
2	Unconformity is onlapped by parallel, semi-continuous reflections	parallel, semi-continuous reflection	parallel, semi-continuous reflections	parallel, semi-continuous reflections	Absent but present in Murombe well as Barremian age	Absent but present in Murombe well as claystone, limestone and sandstone intercalations, Unconformity	HST with retrogradation	The basin is filled by shallow marine clayey siltstones topped by an organic-rich level	The basin is filled by shallow marine clayey siltstones topped by an organic-rich level	The basin is filled by shallow marine clayey siltstones topped by an organic-rich level

Unit/ Surface	Main characteristic	Seismic facies Shelf	Seismic facies Slope	Seismic facies Basin floor	Tentative correlation with well 2012/13-1 (ages, SBs, MFS)	Lithology in well 2012/13-1	Interpretation of unit/surface	Lithology prediction Shelf	Lithology prediction Slope	Lithology prediction Basin floor
3	Unconformity is onlapped by parallel, semi-continuous reflections; a well-marked downlap surface at the top interpreted as a second-order MFS; Retrogradation near shelf (eastern)	parallel, semi-continuous reflection	Parallel, Continuous reflections	parallel, semi-continuous; sub-parallel wavy reflections	Absent but present in Murombe well as Aptian age	Absent but present in Murombe well as dark grey, organic, shales	HST; Top is mfs With retrogradation	The basin is filled by shallow marine clayey siltstones topped by an organic-rich level	The basin is filled by shallow marine clayey siltstones topped by an organic-rich level	The basin is filled by shallow marine clayey siltstones topped by an organic-rich level

Unit/ Surface	Main characteristic	Seismic facies Shelf	Seismic facies Slope	Seismic facies Basin floor	Tentative correlation with well 2012/13-1 (ages, SBs, MFS)	Lithology in well 2012/13-1	Interpretation of unit/surface	Lithology prediction Shelf	Lithology prediction Slope	Lithology prediction Basin floor
4	Downlapping on unit 3; Progradation near shelf (eastern); coastal onlap parallel as compared to unit 3 ;	well-formed clinoforms (oblique) below the shelf, parallel-subparallel reflection	Parallel, Continuous reflections; progradational downlap	sub-parallel wavy reflection	Albian age	Claystone, Silty Claystone	LST/TST with progradation near shelf	carbonate platform deposits for clinoform	Claystone; silty claystone	Claystone; silty claystone

Unit/ Surface	Main characteristic	Seismic facies Shelf	Seismic facies Slope	Seismic facies Basin floor	Tentative correlation with well 2012/13-1 (ages, SBs, MFS)	Lithology in well 2012/13-1	Interpretation of unit/surface	Lithology prediction Shelf	Lithology prediction Slope	Lithology prediction Basin floor
5	progradational downlap ; sigmoid clinoform;	Onlap onto the coast-parallel hinge line; well-formed clinoforms (sigmoid) below the shelf	progradational downlap	Low amplitude semi parallel reflector	Cenomanian age; mfs at early age	Limestone, Claystone, Silty Claystone	Progradation; LST; onlap; mfs at early; aggradational wedge, continuous parallel reflectors; HAC	Claystones; rare siltstones ; sandstones interbeds	Limestone, Claystone, Silty Claystone	
6	progradational downlap; sub-parallel slightly disrupted; low-angle clinoforms stacked in an aggradationa	sub-parallel slightly disrupted progradational downlap; sub-parallel slightly disrupted	progradational downlap; sub-parallel slightly disrupted	Low amplitude semi parallel reflectors	Turonian age; mfs at early age	Claystone, Silty Claystone, Limestone and trace Chert	clayey basin-floor fan; max of accommod at of margin			

	l trend; maximum sediment accommodation									

Unit/ Surface	Main characteristic	Seismic facies shelf	Seismic facies Slope	Seismic facies basin floor	Tentative correlation with well 2012/13-1 (ages, SBs, MFS)	Lithology in well 2012/13-1	Interpre tation of unit/surf ace	Lithology prediction Shelf	Lithology prediction slope	Lithology predictio n basin floor
7	progradational to aggradational wedge	progradational downlap	progradational downlap		Santonian age;					
8		progradational downlap; sub-parallel slightly disrupted	progradational downlap; sub-parallel slightly disrupted	Low amplitude semi parallel reflectors	Campanian age; erosive unconformity, sequence boundary	Claystone, Silty Claystone, Limestone and trace Chert	clayey basin-floor fan	Claystone: siltic, sandy in part and thin layers of sandstone	Claystone, Silty Claystone, Limestone and trace Chert	

Unit/ Surface	Main characteristic	Seismic facies shelf	Seismic facies Slope	Seismic facies basin floor	Tentative correlation with well 2012/13-1 (ages, SBs, MFS)	Lithology in well 2012/13-1	Interpretation of unit/surface	Lithology prediction on Shelf	Lithology prediction on Slope	Lithology prediction on basin floor
9	Slope fan; Canyon incisions; chaotic; progradation-aggradation wedge; incised valleys; erosional truncations	sub-parallel slightly disrupted; progradation	progradational downlap; slope fan; chaotic; incised valleys;	Chaotic; incised valleys;	Maastrichtian age; late age unconformity; mfs	Claystone, Silty Claystone, Sandstone and Dolomite	HST LST TST late age unconformity; mfs	Claystone	Claystone, Silty Claystone, Sandstone and Dolomite	

Appendix 3: Non-Interpreted seismic dip line ION-GXT NAM-3000_pstm_stk_20150710 that was used for the study.

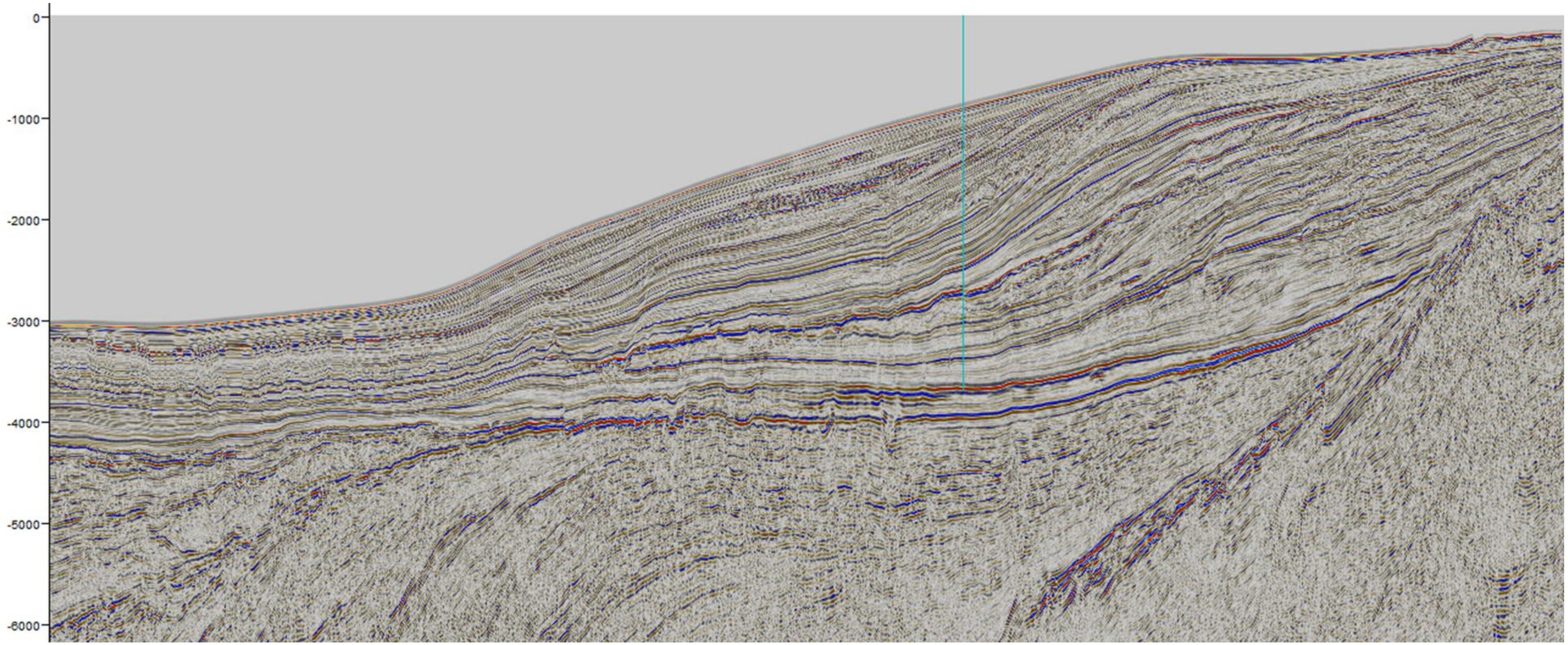

Appendix 4: The seismic dip-line in the Walvis Basin displays reflector terminations mapping. Red arrows show downlaps marking the lower sequence boundary. Black arrows show toplaps marking the upper sequence boundary. Blue arrows show onlaps. System tracts shown as HST (highstand system tracts); LST (lowstand system tracts); and TST (transgressive system tracts). The parasequence sets shown as P (progradation); A (aggradation); and R (retrogradation). The maximum flooding surface is shown as mfs.